Materials Today Physics 15 (2020) 100255

Contents lists available at ScienceDirect

Materials Today Physics

journal homepage: https://www.journals.elsevier.com/materials-today-physics

Additive manufacturing of soft magnets for electrical machines—a review

T.N. Lamichhane [a, **], L. Sethuraman [b], A. Dalagan [a], H. Wang [a, c], J. Keller [b], M.P. Paranthaman [a, c, *]

[a] Chemical Sciences Division, Oak Ridge National Laboratory, Oak Ridge, TN, 37831, USA
[b] National Wind Technology Center, National Renewable Energy Laboratory, Golden, CO, 80401, USA
[c] The Bredesen Center, The University of Knoxville, TN, 37966, USA

ARTICLE INFO

Article history:
Received 19 May 2020
Received in revised form
24 June 2020
Accepted 4 July 2020
Available online 15 July 2020

Keywords:
Soft magnetic materials
Additive manufacturing methods
Electrical motors
Magnetic properties
Multimaterials

ABSTRACT

With growing interest in electrification from clean energy technologies, such as wind power and use of pure electric powertrains in various applications, the demand for next-generation, high-performance magnetic materials has risen significantly. Electrical machine design for these applications is facing challenges in terms of meeting very demanding metrics for power densities and conversion efficiencies, thereby motivating the exploration of advanced materials and manufacturing for the next generation of lightweight ultraefficient electric machines. Additive manufacturing (AM), a layer-by-layer three dimensional (3D) printing technology, opens up new venues of improvements for industrial manufacturing of electrical machines via near-net shape printing of complex geometries, reduction of parts count and production lead time, and conservation of expensive critical materials such as rare-earth magnets as well as nanocrystalline and amorphous soft magnetic composites, allowing their use in only critical regions required by desired properties of the printed parts. The magnetic, electrical, thermal, and mechanical properties of the magnetic materials are also greatly influenced by the selection of the AM method. Among the seven major American Standard Testing and Materials-defined standard modes of 3D printing, selective laser melting, fused deposition modeling, and binder jetting technology dominate the AM processing of soft magnetic materials and their integration in electrical machines. In this work, the state of the art in printability and performance characteristics of soft magnetic materials for electric machines is summarized and discussed. The prospects of soft magnetic materials selection in terms of price, printability, weight, and performance of the electrical machines are also discussed. This review highlights the current status of AM of large electrical machines, AM process selection guidelines, hybrid printing technologies, and the associated opportunities and challenges. An emphasis is put on multi-material processing that is essential for electrical machines. Hybrid printing technologies that combine multiple AM processes with adequate automation and enable simultaneous multimaterials dispensing, real-time quality control, postprocessing, and surface finish with integrated subtractive computer numeric control machining are the requirements for progressing toward the end-user electrical machines.

1. Introduction

In recent years, there has been a growing need for high specific power electrical machines for a wide range of applications including transportation [1] (e.g. hybrid/electric traction, aerospace, marine) and renewable power generation, especially from wind. More electric drone and all-electric passenger aircraft [2] pose challenges, with extensive requirements in terms of specific power, efficiency, safety, and environmental sustainability. In naval applications [3], maximizing revenue for commercial ships and more space to carry mission-critical components for military ships are motivations for higher power density designs for electrification components. On the other hand, minimizing the costs of wind

* Corresponding author.
** Corresponding author.
E-mail addresses: lamichhanetn@ornl.gov (T.N. Lamichhane), paranthamanm@ornl.gov (M.P. Paranthaman).

https://doi.org/10.1016/j.mtphys.2020.100255

power generation requires substantial improvements in specific torque, efficiency, and capital costs [4]. Most of these industries are targeting aggressively lightweight electric machines that cannot be realized using current state-of-the-art electric machine design and manufacturing technologies. Particularly for large wind turbines, even the most optimally designed, low-speed, and direct-drive generators still have physically larger dimensions and weights than desired. For instance, the radial-flux, direct-drive, permanent-magnet generator of General Electric's 12-megawatt (MW) Haliade-X measures approximately 11 m in diameter, contributing to a nacelle weight of over 600 metric tons [4]. Because of the complexity, safety challenges during assembly (e.g. manual handling of magnets or huge back electromotive forces with the slightest rotor movement) and need for specialized equipment for assembly, lifting, and transportation, these generators are factory-preassembled as a large, complete system and most likely also preinstalled within the wind turbine nacelle for transport to the installation site. Hence, there is a need for a lightweight, direct-drive electric generator realized using optimized manufacturing tooling, high-performance low-cost magnets, and steel parts derived from non-critical materials.

Most modern electric machines are inherently complex components with elements made from dissimilar materials with different functionality, stipulated performance, and strength requirements; so, disruptive changes in design have been relatively difficult to achieve using traditional manufacturing. Typically, electric machines employ highly magnetically permeable, soft ferromagnetic materials such as steel or magnetic iron in idealized geometries for shaping and guiding the magnetic fields and providing an effective medium for energy transfer. The most common magnetic material used for this purpose is stacked laminations of thin sheets (0.1–0.5 mm thick) of non-oriented electrical steel. Typical material parameters that are considered during the material selection process for an electric machine core are high magnetic saturation and permeability; low coercivity, specific power losses, and magnetostriction; high yield strength; and resilience to thermal cycling. Functionally applicable soft magnetic materials for motors are typically ferrosilicon (Fe–Si) alloys [5–7].

For a given power rating, the power density of an electrical machine is determined by the magnetic saturation of the material, and hence a higher magnetic saturation is often desired so that it results in less material required to guide the magnetic flux inside the machine core. As the core experiences periodic magnetization and demagnetization cycles, some portion of the energy is dissipated as iron losses and the rest from the expansion and contraction of the material associated with the magnetostriction effect. Because the energy loss greatly impacts the efficiency, the material should exhibit narrow hysteresis behavior and high electrical resistivity. To realize these properties, soft magnetic materials are alloyed with other materials and heat treated to optimize microstructures. This process introduces defects, grain boundaries, and impurities that hinder magnetic domain wall movement and significantly impair magnetic properties. Fig. 1a and b shows the conventional production flow chart for the magnetic core of a motor [8,9]. The process begins with the development of a detailed computer-aided design (CAD) drawing of the machine core that will be carefully assessed to identify and develop special precision tooling for cutting and punching dies for mold forming and stamping. Fe–Si sheets are then cold rolled to the required thickness for lamination and cut to required dimensions. The sheets are coated with insulating material that resists the flow of eddy currents. Stamping and punching shape the sheets to the required geometry. The sheets are then stacked on an aligning fixture by pinning or welding. As part of the quality assurance, the stacks generally require postmachining and heat treatments to prevent deterioration from stresses caused by stamping, welding, and interlocking as described in Fig. 1b. In a conventional process, several laminations are individually stamped, stacked, measured, die cast, lathed, and finished in separate processes. As a result, labor and production times can be significant. Considering the multiple steps and touch-times, some manufacturers have introduced some level of automation for punching, stacking, and lamination that can reduce the labor by 35%–40% [10].

A pictorial display of automated manufacturing steps and manpower reduction in electric stator and core manufacturing in Mitsui High-Tec Inc. is demonstrated in Fig. 2 [10]. Additive manufacturing (AM) can contribute both in parts count reduction and automation. Laminations produced by traditional processes for highly efficient and highly dynamic electric motors still exhibit appreciable losses. The use of thinner laminations can minimize the core loss; however, thinner material requires more steps of rolling, further stress relief annealing, and more laminations for a given stack height, making it more expensive to fabricate [5]. Further, excessive rolling increases the brittleness of steel, imposing a practical lower limit on the available thickness for laminations (about 0.1–0.5 mm thick). A second key limitation is the loss of dimensional accuracy resulting from burrs and warps caused by stamping and stacking operations. An alternative to stamping is wire electrical discharge machining (EDM); however, this increases the tooling cost and consequently requires a large production volume to justify that cost. Further, significant waste results when laminations are shaped into complex designs.

Materials with higher Si content (e.g. Fe-6.5Si) partially offset some of these challenges with increased resistivity; however, they are still limited in their ductility and thermal conductivity. Aside from the losses, the mechanical stability of the structure is of great importance to larger electric machines, especially for aircraft and wind power in which weight is an important consideration. Most Fe–Si sheets have a density of approximately 7,800 kg per cubic meter (kg/m^3), whereas iron-cobalt (Fe–Co) sheets have densities around 8,120 kg/m^3, thus making the electrical machine heavier; however, the high saturation magnetization of Fe–Co alloy over-compensates for this effect and reduces the weight by up to 25%. Usually, this disadvantage is countered by the fact that these sheets have a high saturation magnetization, so less material is needed to create the same amount of magnetic flux [2]. However, for high specific power and torque applications, these laminations must provide the same magnetic flux but with lower material in the yokes and teeth. Therefore, there is need to change the way electric machines are designed and manufactured, and AM can certainly address some of these needs.

As new materials processing methods continue to emerge, electric machine designers are constantly looking for better-performing manufacturing techniques that provide greater design freedom. In recent years, the growing availability of magnetic materials with new compositions and material processing through AM techniques, such as three dimensional (3D) printing, are opening up a new opportunity for designing electric machines. AM is a layer-by-layer material addition technology to fabricate desired parts [11,12]. It has the ability to produce machinery parts of complex geometries or unify parts to reduce the complex parts count [13,14] and advanced functionalities without the need for complicated tools and molds. It can facilitate the manufacturing of gigantic machines at the installation site and avoid shipping and installation complications. An example is multi-MW wind turbines, whose highway shipping size is constrained by overhead bridges. AM can significantly decrease the materials requirements for the parts production. In the language of AM, it increases the buy-to-fly ratio, allowing the purchase of higher-grade feedstock for the same price. Similarly, in soft magnetic materials manufacturing, AM can

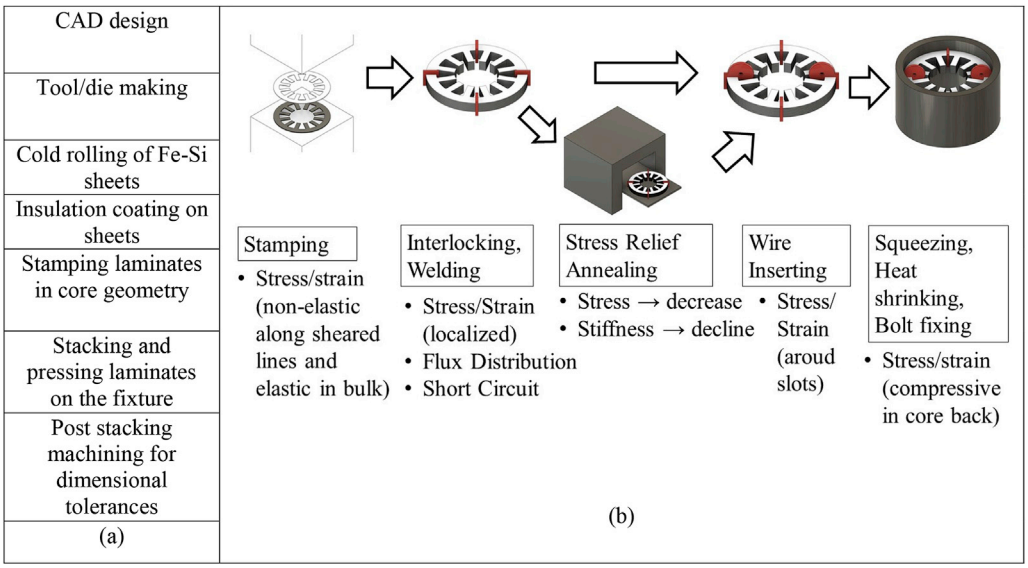

Fig. 1. (a) Steps in traditional manufacturing process [8] and (b) its demonstration for a motor core adapted from Ref. [9] illustrating the deterioration process in manufacturing. CAD, computer-aided design.

provide the freedom of choice of material grade only on the selected region of the part to control price and physical properties. For example, AM can open up the possibility of using various lamination thicknesses in electrical cores, teeth, and yokes [15]. Similarly, AM can not only provide the net-shaping of complex machine parts but also can facilitate the processing of higher quality alloys. Babuska et al. [16] recently reported improvements in tensile strength and ductility in additively manufactured Fe—Co alloy. AM has shown a greater potential than conventional manufacturing to improve the functionalities of manufactured parts and components in various applications such as medical, aerospace, and electrical industries. Finally, AM can also facilitate the repair and maintenance of large machine parts like turbine blades and airplane propellers. The AM process for an electric machine core begins with generating a prototype model using CAD software and implementing the 3D printing using feedstock materials. Flowcharts are convenient in process demonstration in AM [17—19]. A typical flow chart for AM of electric machines is shown in Fig. 3. The wiring and cabling steps in AM of electrical machines can be avoided if unconventional shapes of inductors [20,21] and other passive components such as cores with complex cavities [22], axial flux permanent magnet (PM) motors [23], and individual components of soft magnetic composite (SMC) [24] are considered. Implementing a stringent quality control method for every step of the manufacturing process is extremely important. Some examples include the use of a closed loop defect control mechanism using image analysis for fault detection and correction [25], machine learning (ML) supervised process control [26], camera enforced 360° real-time process monitoring [27], computerized tomography, etc. Such mechanisms will also be very essential in electrical machine printing which could potentially reduce the rate of defective parts.

AM is continuously evolving with the advancement of printing technologies; however, because of the necessity of the use of hard and soft magnetic materials in electrical machines along with copper wire insertion, a single step fabrication of electrical machines is still a challenging future goal. An obvious advantage offered by AM is the elimination of multiple processes resulting in substantially faster production times for machine cores. For example, manufacturing a stator plate using machining or EDM and milling processes is estimated at over 4 months, while 3D printing would provide the same part within 1 week, as shown in Fig. 4 [28]. The absence of traditional tooling and processing is expected to reduce fabrication costs significantly.

Because AM can enable easy printing of thin-walled hollow structures of new materials [8] with high electrical resistivity, it offers excellent potential for core loss reduction. Even complex core designs can be realized; for example, continuous skewing, complex flux paths with integrated cooling channels [9], can result in better performing designs with substantial cost and weight savings with reduced waste of critical materials. Further, because AM allows a mix of different types of metal powders, higher-quality alloys, and the inclusion of binding agents, improved material properties are possible by controlling grain texture and the grade of soft magnetic materials in specific sections of the machine parts [29]. Because AM can process both soft magnets and insulation materials, it may be possible to realize fabrication of cores using multimaterial printing. Brief details of the prospective of multimaterial AM of electrical machines is discussed later in the outlook section.

A review of the most recent literature in AM for electric machines suggests different levels of technology maturity [30—32], with most of the research aimed at qualifying advanced ferromagnetic alloys for realizing design complexities or new geometric features that cannot be made by conventional manufacturing and result in substantial weight reduction. Many of the efforts have been focused on developing materials with suitable electromagnetic properties using a variety of methods, including selective laser melting (SLM), fused deposition modeling (FDM), and binder jetting technology (BJT). Other reported processes include cold spray (CS), spark plasma sintering (SPS), stereolithography (SLA)/ digital photolithography (DLP), and laminated object manufacturing (LOM). In these methods, the printing quality was found to be extremely sensitive to process parameters. A team of researchers from the National Research Council (NRC) Canada [33] undertook the first efforts to redesign and print an electric motor enabled by CS and fused filament fabrication (FFF) techniques. While the magnetic core material developed using FFF techniques resulted in a lesser volume fraction, the density and permeability values reported for CS-processed core material were comparable to compacted SMC, and the redesigned motor was found to exhibit

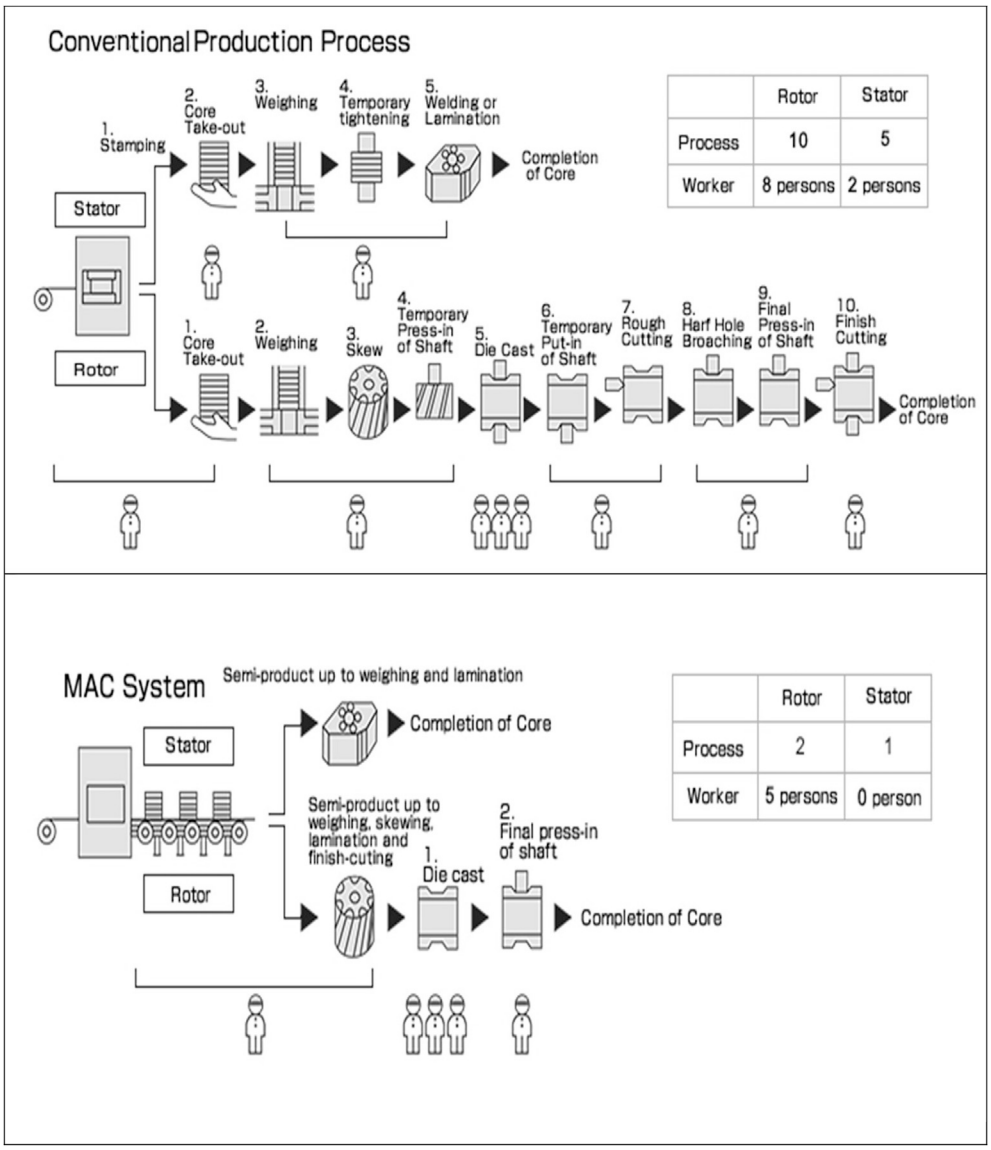

Fig. 2. Comparison of process flow charts for conventional production process and automated 'Mitsui Automatic Core assembly system' from Mitsui High-Tec Inc. (printed with permission) [10].

higher torque and efficiency. Apart from conventional iron alloys, there have been ongoing efforts to explore printing techniques for SMCs [34,35]. The basis for SMC is the use of iron particles coated with a thin insulating material that separates each particle, offering very high resistivity to eddy currents. Wu et al. [32] proposed a fully additively manufactured PM machine with a modular stator encapsulated by SMC cores that acted as an elaborate heat exchanger for the windings as well as for the power electronics. They also highlighted opportunities for optimized magnet shapes, simplification of the rotor manufacturing process, and effective cooling for the rotor. Several other research efforts [35–37] focused their attention on additive designs and printed soft magnet materials for motors. A detailed material evaluation has not been reported to verify the suitability of any of the above processes and studied materials for large-scale soft magnetic core fabrication for electric machines. A promising application that would greatly benefit from these developments in soft magnet AM is large-size multi-MW direct-drive generators that bring along their own challenges in material costs, manufacturing, transportation, and site installation [38]. Being dimensionally much larger and operating at higher torque than many other applications, both the magnetic and mechanical properties play a vitally important role in the material selection process for these machines that are currently dominated by high-silicon (Si) steel and SMC.

During the last decade, the growth in wind power generation has greatly increased the demand for new and advanced high specific power generators. A variety of next-generator designs that are starting to emerge employ advanced soft magnetic electrical parts with reduced electric losses and improved mechanical strength, necessitating the use of newer and advanced manufacturing technologies. The electrical steel in the rotor of these generators is exposed to particularly high mechanical stresses from operational loading, which necessitates substantial use of high-strength material besides also satisfying the basic functionality of flux guiding. Higher magnetizability and a higher thermal conductivity compared with currently available soft magnetic materials for rapid heat dissipation can enable newer designs with higher efficiency at a smaller size. AM can provide a pathway

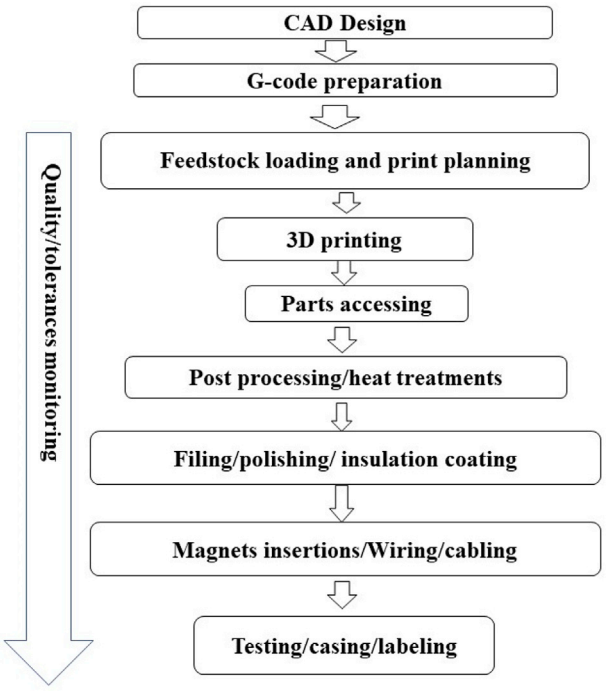

Fig. 3. General flowchart for AM manufacturing of electrical cores. CAD, computer-aided design; AM, additive manufacturing.

for realizing new design freedom that results in the most optimal use of materials and weight and, in the future, enable on-site manufacturing of large generators that can also help decrease shipping, transportation, and handling costs and increase the production rate. If mechanical integrity is of significance, a solid iron core could be realized by laser beam melting (LBM); however, because the cohesive bond between layers is based on re-melting previous layers, a higher shear stress on the rotor core can result in non-uniformity and heterogeneity at a microscopic level [35,36]. Published research considering the potential of AM for power density improvements for wind turbine generators is scarce, but an obvious opportunity remains to be explored considering the progress made in some of the ongoing research efforts in soft magnet printing that suggest a better future for electrical machine manufacturing.

In the remainder of this article, we provide a critical review of the state-of-the-art 3D printing technologies for soft magnets, uncovering new challenges when applied to large-scale industrial printing and the potential outlook in the field to realize full-fledged, multimaterial AM of electrical machines.

2. Survey of major soft magnetic materials

All the traditionally utilized soft magnetic alloys (namely Fe−Si, Fe−Ni, Fe−Co, and SMCs) are the candidates for AM in electric machines [39]. Soft ferrites are only integrated in transformer and antenna and are not easily integrated in rotors because of their low magnetization and brittleness. However, AM will open up the processing methods even for brittle materials, and the higher electrical resistance of the soft ferrites makes them alternative candidates for insulating materials in electrical cores. In this section, we discuss these soft magnets, including ferrite's brief history of alloy development, materials composition, and associated market brands, processing parameters for electrical core formation and their effect in magnetic, thermal, mechanical, and electrical properties. We will also qualitatively discuss the suitability of their applications in electrical machines in specific frequencies and temperature ranges. We start from the basic terminologies for the soft magnetic materials that are essential for understanding of their use in stipulated applications. The key parameters for soft magnetic materials are saturation magnetization (M_s), coercivity (H_c), remanence (B_r), relative permeability (μ_r), electrical resistivity (ρ), thermal conductivity (k), and mechanical strengths. To understand the magnetic parameters, we take reference of a typical bulk Fe−3Si sample magnetization data as presented in Fig. 5a−d.

Fig. 5a shows the room temperature $M(H)$ and $B(H)$ data, which includes a small hysteresis loop enlarged in Fig. 5b. The magnetization induction B is related with magnetization M as $B(T) = \mu_0(H+M)$. Here $\mu_0 = 4\pi \times 10^{-7}$ H/m, and H and M are measured in A/m in the SI system. The X-intercept of the linear fit of first quadrant of $M(H)$ and $B(H)$ data at higher field region provides the saturation magnetization M_s as shown in Fig. 5b. To increase the M_S, the presence of larger grains in ferromagnetic materials are essential. The Y-intercept of linear fit $B(H)$ data in the second quadrant of provides the remanence B_r for the materials. In soft magnetic materials, B_r is very small (~0.02 T) as shown in Fig. 5c. The remanence in hard magnetic materials that are used for PMs could be up to 0.9 M_s. In case of single crystalline PMs, it could be ideally as big as M_s[40]. The virgin magnetization in the first quadrant (red data points) is increasing much slower than the fifth quadrant magnetization because of static demagnetization effect in the sample, which ultimately collapses with fifth quadrant data followed by Barkhausen noise in the ferromagnetic materials. This effect is also visible in some hard ferromagnetic materials [41]. The X-intercept of the magnetization data provides the coercivity (H_c) of the magnetic materials. The smaller the hysteresis loop, the smaller the electrical core loss will be in electrical machines. The last and one of the key parameters that can be extracted from the magnetization data is relative permeability (μ_r) which is magnetic

Fig. 4. NASA's comparison of fabrication times and costs for a stator plate [28].

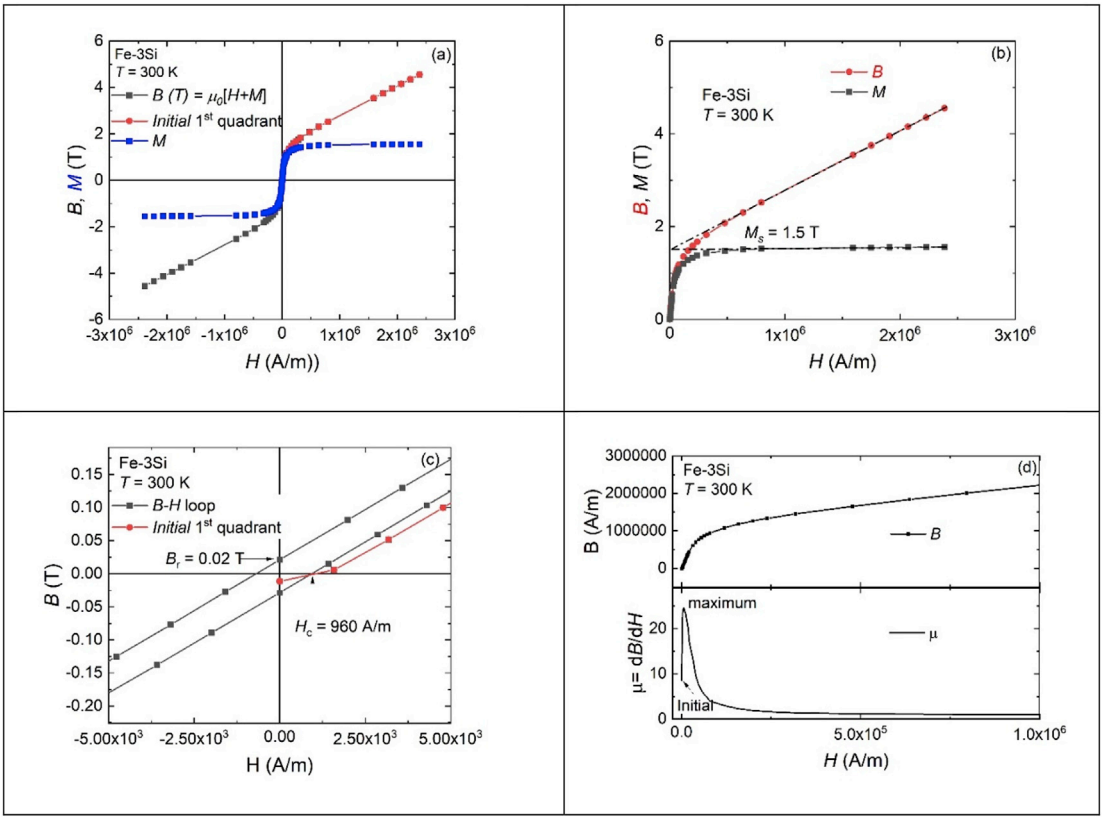

Fig. 5. (a) Room temperature magnetization data *M(H)* and *B(H)* loops for a standard Fe−3Si; (b) Determination of saturation magnetization M_s; (c) Explanation of remanence B_r and coercivity H_c; and(d) Extraction of permeability of soft magnetic materials.

field derivative of magnetic induction for the first quadrant ($\mu_r = dB/dH$) as shown in Fig. 5d. The initial permeability is the slope as $H \rightarrow 0$, and maximum permeability corresponds to the maximum slope peak. The maximum permeability peak corresponds to the maximum flux guidance capacity of the material at the corresponding field.

Apart from the magnetic properties, electrical and mechanical properties are the key parameter for the soft magnetic materials. The high electrical resistance helps to suppress the eddy current in the soft electric cores. The electrical resistance mainly determined by the material's band structure which can be controlled by the addition of Si, a cheap semiconductor material, to Fe. In addition to the increase in electrical resistivity, Si doping also decreases the magnetic anisotropy. The decrease in magnetic anisotropy helps to increase the permeability in high Si steel. Additionally, magnetostriction parameter (λ), the extension and contraction of magnetic cores with applied field, also decreases significantly.

The magnetostriction, permeabilities, and electrical core losses are complex functions of electrical signal frequencies [42–47]. The simplest understanding of magnetostriction is vibrational noise associated with the shape of the electrical core. As magnetization tends to saturation, harmonic effects are produced and electrical losses increase with additional noise [42]. One can assume signal frequency as a driving force for non-linearity in the nature of vibration. It also depends on magnetic and shape anisotropy of magnetic materials. Both the anisotropic and rotational magnetostriction phenomena in electrical steel are explained in detail in the literature [45].

To understand the effect of electrical signal frequency in permeability, it is convenient to start from the response of passive elements in an electric circuit where phase shift is associated with electrical loss. Similarly, if the induced magnetization does not follow the magnetizing field phase, frequency, and amplitude, the magnetic susceptibility can be expressed as a function of frequency using

$$M(\omega) = \chi(\omega) H(\omega) \tag{1}$$

Where $\chi(\omega) = \chi' + i\,\chi''$ is complex susceptibility which is related to permeability as

$$\mu(\omega) = \mu' + i\,\mu' = \mu_0(1 + \chi(\omega))$$

The relationship of all of these frequency-dependent quantities to electrical loss and machine size can be further understood from Faraday's law of electromagnetic induction, the induced EMF (E) in a soft magnetic material is accounted with the formula

$$V = -\frac{\mu N^2 A}{l} I_0 \omega \cos(\omega t) \tag{2}$$

where the symbols stand as μ (permeability), N (turns), A (wire cross section) l (the core length) I_0 (signal amplitude), and ω (signal frequency) [44]. For a given material (of certain permeability) in the maximum induction condition ($\cos(\omega t) = 1$), the cross-section (size) of the device is inversely proportional to frequency i.e.

$$A_{device} \propto \frac{1}{\omega} \tag{3}$$

Thus, materials with high permeability at high frequency are desirable for realizing smaller machines at higher power rating. This suggests that soft ferrites could be ideal candidates; however, their low magnetization, thermal conductivity, and brittleness (see

Table 3 below) are precluding their selection. AM can facilitate the processing of such brittle, high frequency permeable soft magnetic materials in electrical machine manufacturing along with arrangement of cooling mechanism such as liquid and gas flow channels.

Most popular soft magnetic material families based on primary alloy elements that are extensively used in different forms such as compact powder, laminated sheets, nanocrystalline, soft composite, and/or amorphous forms are presented in Table 1, and their major magnetic properties are presented in Fig. 6. Out of these major categories of soft magnetic materials, there are also subcategories of commercial grade materials with specific commercial names and properties, such as permalloy and supermendur, included in subcategories of Table 1. Because of patent rights, the commercial soft magnetic materials are often sold under trademark names with specified performance rather than actual compositions [46]. Fig. 6 shows the saturation magnetization and permeabilities for the seven major soft magnetic families. These two key parameters can provide a quick reference guide regarding which soft magnetic materials could serve for a specific application. The properties of the bulk powder materials are useful for high magnetic induction (saturation magnetization), whereas they provide only lowest relative permeabilities, which is a key desired property for the soft magnetic materials. For example, the 50:50 Fe–Ni powder core provides a low permeability (a few hundred [47]), which suddenly increases to 100,000 times for the permalloy (~80% Ni:20%Fe) followed by appropriate heat-treatment to achieve the desired microstructure [48]. Thus, the processing modes, such as heat treatment [48], purity of ingredients [49], and microstructure development, as well as appropriate postprocessing in AM manufacturing technologies [16] play a significant role in the improvement of magnetic properties of the soft magnetic materials. The major steps in preparation of electric cores such as cutting, punching, stamping, and stresses associated with them influence the various physical parameters of soft magnetic materials as shown in Table 2.

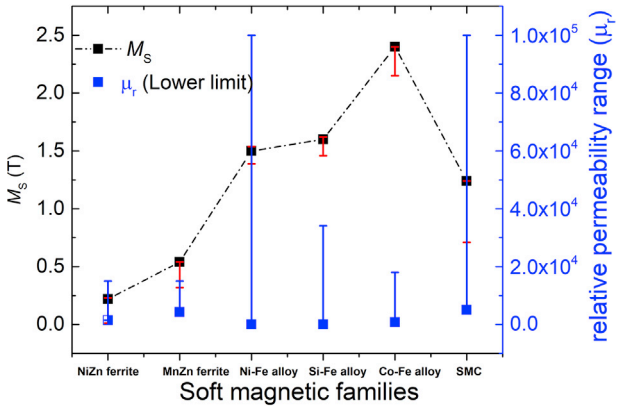

Fig. 6. Classification of industrial soft magnetic materials based on primary constituent of the alloys and their saturation magnetization and available range of relative permeabilities (SMC: soft magnetic composites). The deviations in saturation magnetization (red symbols) and permeabilities (blue symbols) depend on the ratio of primary elements, methods of preparation, and additive elements. For detailed explanation, please see the text in the respective sections. (For interpretation of the references to color in this figure legend, the reader is referred to the Web version of this article.)

As casting followed by hot and cold rolling are the traditional processing techniques of electrical materials and tool steels, phase segregation and crystallographic texture in soft magnetic materials limit their applications. The major limitations of the casting technology are the lack of control in grain boundary engineering and isotropic nature of microstructures, which are needed for rotor applications. To overcome this limitation, the powder metallurgy process utilizes isotropic particle distribution and optimizes the sintering and heat treatment cycles, which in turn optimizes the

Table 1
Partial list of various commercial soft magnetic materials; quantitative and qualitative measure of their appropriateness for electric machines.

Material families		Saturation magnetization M_s (T)	Relative permeability μ_r	Core resistivity $\rho(\mu\Omega cm)$	Material density (g/cc)	AM modes/types[a] [References]
Ferrites	$MnZnFe_2O_4$	0.32 to 0.545	350 to 20,000	10^7 -3 × 10^9 [50]	–	–
	$NiZnFe_2O_4$	0.22 to 0.42	15 to 2,000	(1.26–6.84) × 10^{11} [51]	–	FDM [52] FDM + UV cure [53]
	$CoZnFe_2O_4$	0.103	1.94	0.288 × 10^{10} [54]		–
Fe–Ni based alloys	Molypermalloy (MPP) [47,55] ~(81% Ni-17% Fe–2% Mo)	0.7	14 to 550	60 [39]	8.2	–
	High flux [47] (50% Ni–50% Fe)	1.5	14 to 160			–
	Permalloy/(Mu-metal) (~80% Ni–20% Fe)	1.08	8,000 to 120,000 [48]			SLM [56,57],
	Supermalloy [55,58],	0.66 to 0.82	40,000 to 100,000			SLM [59,60],
Fe–Si based alloy	Fe–3%Si	2.15	25	20–60 [39]	7.34	SLM [61]
	Fe-6.5Si	1.8	10,700	82 [39]	7.3–7.7	BJT [62]
	Sendust/Super-MSS [47,63], (Kool Mμ) 85% Fe- 9% Si–6% Al	1.0	14 to 125	–	–	–
Fe–Co based alloy	Permendur (Supermendur) [49]/ Hyperco [64] 49% Fe-49% Co–2% V	2.4	20,000 to 66,000	40 [39]	8.12	SLM [16,64,65],
SMC and other soft magnets	Amorphous Iron 20% (Si + B) 80% Fe [39]	1.55		130 [39]	7.18	
	SMC <1% lubrication, Fe balanced [39]	0.71–1.22		20,000 [39]	7.57	SLM [66]
	FINEMET (glass) ~$Fe_{73.5}Si_{13.5}B_9Nb_3Cu_1$	0.53 to 1.24	6,000 to 100,000	130 [39]	7.18	SLM [67,68]
	Metglass ($Fe_{80}Si_9B_{11}$) [69]	0.57 to 1.51	20,000 to 1,000,000	130 [39]	7.29–7.9	[a]

SMC, soft magnetic composite; FDM, fused deposition modeling; SLM, selective laser melting; BJT, binder jetting technology; AM, additive manufacturing.
[a] Metglass exhibits ultra-high permeability because of field annealing and is not included in Fig. 6 for visualization.

Table 2
Various influencing factors on physical properties of soft magnetic materials for electrical cores.

Influencing factor	Permeability μ	Resistivity ρ	Thermal conductivity k	M_s	H_c	P_{hyst}	P_{ec}	P_{exc}
Grain size (d_{grain} ↑)	↑	↓	↑	↑	↓	↓	↑	↑
Sheet thickness ($_d$ ↑)		↓	↑		↓	↓		
Internal stress (↑)		↑	↓		↑	↑		
Cutting/punchingprocess (↑)						↑		
Additives (↑)		↑	↓		↑	↑		
Pressing/stamping (↑)	↑			↑	↑	↑		
Heat treatment	↑	↓	↑	↑	↓	↓		

grain boundary and microstructures and improves the mechanical and electrical properties. High efficiency, lightweight electrical machines require high-quality feedstock materials and involve complex geometries that are not possible in conventional powder metallurgy manufacturing techniques. Challenges remain in complex part formation and the need for special tools for molding/pressing and assembly. Further, powder metallurgy and its assembly are energy-demanding technologies. To overcome these limitations, AM can facilitate feedstock formation, tool free designs, and parts count reductions and can achieve complex architectures of electrical machines.

The selection of materials for electric machines involves a careful tradeoff among their desired properties (magnetic, mechanical, and thermal) and costs for the best performing designs [70]. A literature survey [6,71] highlights some of the physical and manufacturing factors that influence the main properties for lamination sheets made from soft magnet materials, as illustrated in Table 2, in which the inclined up and down arrows represent the increase and decrease in the parameters. From the point of view of controlling iron loss by hysteresis (P_{hyst}), it is desirable to reduce intrinsic coercivity and the area contained within the hysteresis loop. Eddy current losses (P_{ec}) and excess loss associated with domainwall motion (P_{exc}) can be reduced by thin laminations that offer greater resistance to skin effects at higher frequency. The use of homogeneous material and larger grain size with control over impurities, such as carbon (C), nitrogen (N), sulfur (S), oxygen (O), and boron (B), can prevent hindrance to the domain wall displacement and together with higher alloy content can greatly improve saturation magnetization (M_s); however, it decreases the coercive field (H_c). Traditional approaches to achieving improvements are limited, especially in alloying content. With AM, it is likely possible to achieve a better control over alloy content, grain size, and eliminating undesirable second phase impurities from annealing treatments. Based on the survey on additively manufacturable conventional and emerging soft steel for multi-MW electric machines, Table 3 summarizes the appropriateness of the available materials qualitatively. The color codes at the bottom represent the appropriateness of the material parameters for electrical machines—red color for unacceptable through green for ideal performance. Besides these candidates, identification of newer soft magnets will be driven by technical needs and innovative designs.

Table 3
Qualitative measure of appropriateness for different soft magnetic materials families for different physical properties and materials technology readiness level (TRL) assessment [70]. The implications of color codes are shown at the bottom.

		Low Frequency	High Frequency	Temperature Stability	Cost	Mechanical Properties	Thermal Conductivity	Bs	Init. Permeability	Resistivity	Material TRL	System TRL
Conventional materials	Low C Steels				Very Low Cost						Commercial	Commercial
	Si Steels										Commercial	Commercial
	NiFe Alloys	Very Low Loss							Very Soft Alloys		Commercial	Commercial
	CoFe Alloys			Highest T_{Curie}				Highest Bs			Commercial	Commercial
Emerging materials	Amorphous Alloys	Very Low Loss			Higher $/kg, But Smaller Volume				Very Soft Alloys	Amorphous	Commercial	
	Fe-Based Nanocomposite Alloys (Conventional)	Very Low Loss			Higher $/kg, But Smaller Volume	Brittle			Very Soft Alloys	Amorphous Matrix	Very Soft Alloys	
	Fe-Based Nanocomposite Alloys (Partially Crystalized)	Very Low Loss			Higher $/kg, But Smaller Volume				Very Soft Alloys	Amorphous Matrix	Very Soft Alloys	
	Co-Based Nanocomposite Alloys				Higher $/kg, But Smaller Volume					Amorphous Matrix		
	Soft Magnetic Composites									Insulating Binder/Matrix		Insulating Binder/Matrix
Could be useful in AM	Ferrites							Lowest Bs			Commercial	

Unacceptable
Low performance
Acceptable
Competent
Ideal

Table 4
Survey of recent literature on soft magnetic materials and their uses in electrical machines.

Printing method	SLM	FDM	BJT	SLA/DLP	CS	SPS
Literature reviewed	28	17	5	3	3	1
Percentage	49%	30%	9%	5%	5%	2%

FDM, fused deposition modeling; SLM, selective laser melting; BJT, binder jetting technology; SLA/DLP, stereolithography/digital photolithography; CS, cold spray; SPS, spark plasma sintering.

Several research efforts suggest significant improvement in magnetic properties by use of appropriate postprocessing modes such as heat treatment [48], purification of ingredients [49], and microstructure control [16]. The brittle, high-Si content Fe–Si alloys and Fe–Co alloys can be easily 3D printed using powder feedstock despite their low workability for the cold rolling. Additionally, ordered chemical phases can be avoided by annealing the printed parts at a temperature slightly lower than the crystallization temperature of the alloys. SMCs have highest resistivity and favorable mass densities; however, their saturation magnetization is greatly reduced. With AM, several of these physical properties are anticipated to improve significantly. Among the conventional and emerging materials listed in Table 3, soft ferrites were considered unsuitable materials for large electrical machines because of their low magnetization, brittleness, and difficulty in machining. Soft ferrites could replace insulating materials in electrical laminates as a small 3D-printed boundary layer between the electrical steel layers. An illustration is purposed for multimaterials processing in the outlook section. Among several available reports on AM for soft magnets and electric machines [30,34,36,50–57,72–80], it is observed that SLM and its variants, including laser powder bed fusion (L-PBF) and laser engineered net shaping (LENS), are the most extensively practiced methods [7,56,67,74,82–88]. This trend is generally associated with appropriateness of laser to process diverse kind of soft magnetic materials. Laser melting generates the dense and mechanically strong parts which also pose high magnetization needed for the electrical machines. Additionally, laser easily can process high melting transition metal-based compounds, such as nickel (Ni), Fe, Co, chromium (Cr), and manganese (Mn) that require refractory metals like zirconium (Zr), hafnium (Hf), tantalum (Ta), titanium (Ti), and vanadium (V) for workability, microstructure generation, hardness, and corrosion resistance. The second more practiced method for soft magnetic materials processing is FDM [77,87–94]. There are few reports on BJT [62,95–97], SLA [91,98], DLP [99], CS [33], and SPS [67]. We conducted an exhausted survey of the literature on the AM of soft magnetic materials and their use in electrical machines manufacturing and presented the statistics in Table 4. As shown in Table 4, SLM is the most practiced method, followed by FDM and BJT. In the following sections, we review the AM status of major soft magnetic materials families, challenges using traditional synthesis, and potential solutions using AM in Section 2 and their use in electrical machines manufacturing in Section 3.

2.1. Fe–Si alloys

Ever since Faraday's demonstration of electromagnetic induction using soft iron in 1831, there has been a continuing evolution of soft magnetic materials. Attempts to improve the properties of soft iron began in 1910 when Robert Hadfield, a metallurgist from England, invented non-oriented Si steel by adding up to 3% Si to iron and increasing its electrical resistivity (ρ) while also increasing its relative permeability [46]. Today, Si steels account for the major share in the rotating electric machine market (as isotropic non-oriented Si steel), with an excellent combination of price and performance for large, industrial-scale applications. Fe–Si alloys with low Si content (Si < 9.5% weight) are the dominant soft magnets employed in various types of electric motor cores because of their relatively high resistivity, near-zero magnetostriction, and low magnetocrystalline anisotropy that is manifested as high initial permeability [100]. More importantly the reasonable commercial price and necessary specific power available for electrical machines made is the most suitable choice material. Presently, the low-Si Fe-alloy, Fe-3.2Si, can be processed with a conventional cold rolling technique and account for almost 90% of the low-frequency electric machines. To be applicable in high-frequency electrical machines, the high-Si content Fe–Si alloy needs to have a high permeability and electrical resistivity. Alloying with higher Si content provides a mass density advantage; however, this is offset by the reduction in saturation magnetization and increase in brittleness of the alloy because of the formation of B_2 and $D0_3$ chemically ordered phases during slow cooling. These phases can be avoided by melt-spinning and rapid quenching of Fe–Si ribbons [101]. The melt-spinning also improves the properties of high-Si (~6.5 at.%) steel [102]. So far, expensive chemical vapor deposition and diffusion siliconizing processes [103] via annealing have been used to avoid these phases in the conventional process and cracking during cold rolling. AM can enable avoiding these phases by printing electrical machine cores using atomized, amorphous Fe–Si alloy powder and annealing the printed part at a lower temperature.

AM of Fe-6.5Si alloys has been attempted using SLM [15,100,104,105] and BJT [62]. However, the sizes of the specimens synthesized using SLM studies have been relevant only for material characterization purposes and not relevant to practical sizes of electrical machines. Goll et al. fabricated toroidal prototypes of 5-mm height using L-PBF, in which the largest toroid had outer/inner diameters of 40/30 mm, respectively [15]. Niendrof et al. synthesized cylindrical samples of anisotropic steel using SLM with dimensions of 10-mm diameter and 65-mm length [81]. Garibaldi et al. reported SLM synthesis of cubic samples of 5-mm sides [100]. Despite the limited lab-scale research in the SLM technique, there are some promising results. These studies did not observe any B_2 and $D0_3$ ordering as a result of the rapid melt quench rate in SLM [101]. The density of Gauss texture was also found to increase with higher laser power [81,100]. The increase in the textured nature of SLM alloy was also observed in $AlSi_{10}Mg$ [82,106]. However, Goll et al. observed more defects and an increase in internal crack densities with higher laser power [15]. It is possible to control defects using a primary laser beam for melting and secondary laser beam to control the microstructure [11]. This highlights a better future for application of AM-based high-Si steel; however, the net shape printing of Gauss-textured steel starting from the precursor powders is an existing challenge. Large part manufacturing with Fe–Si alloys would need high laser energy. At higher energy, there is a tendency for Goss texture to change to cube-texture and an increase in porosity of printed parts because of bulging melt-pool morphology.

2.2. Fe–Ni alloys

In the 1910s, Gustav Elmen at Bell Laboratories experimented with iron-nickel (Fe–Ni) alloys and discovered the Ni-rich alloy called permalloy (with 78.5% Ni concentration). Permalloys are well known to have superior soft magnetic properties in terms of losses, permeability, and magnetic field annealing response [3] and lower saturation induction but are more expensive than Si steels, so fewer implementations in electric motors have been reported [107]. The permeability peaks only at a narrow range of approximately 75%–80% Ni; therefore, most commercial permalloys stay within this

composition. Over time, the definition of permalloys has loosened and is used in certain sources and scientific papers to refer to any Fe–Ni alloy with Ni proportions ranging from 35% to 90% and can include small amounts of other elements [56,108]. Typical commercial samples of permalloy can contain the following composition: Ni 78.23, Fe 21.35, C 0.04, Si 0.03, P trace, S0.035, Mn 0.22, Co 0.37, and Cu 0.10. Proper heat treatment is crucial to obtain permalloys with the highest permeability, and the permalloy must be cooled through proper temperature ranges at proper rates. Supermalloy contains ~79% Ni and ~5% Mo, with the rest being Fe and a small amount of Mn. Heat treatment is also important for supermalloy and both temperature and cooling rate must be optimal to achieve maximum permeability. Supermalloy can have 50,000 to 150,000 for initial permeability and 600,000 to 1,200,000 for maximum permeabilities [58,109]. In contrast, depending on the cooling rate, a permalloy can only have approximately 6,000 to 10,000 for initial permeability and 40,000 to 120,000 for the maximum permeabilities [110].

Permalloys have been successfully utilized in many AM processes because of their exceptional permeability. One such process is directed energy deposition (DED), a powder or wire-fed AM process that does not need a powder bed, unlike other common metal powder AM processes. Mikler et al. successfully used DED to produce a variety of 30% Fe permalloys from a blend of elemental powders, which did not need prealloying as feedstock [60]. Permalloys have also been manufactured by powder bed methods such as LBM. Schönrath et al. successfully created permalloys via LBM of a powder blend of Ni and Fe. Again, the powders are commercially available, high-purity raw materials that have not been prealloyed. They used the standard 78.5% Ni composition with particle sizes in the range of 5–55 microns (mm), with the mean diameter of a Ni particle being 30 mm and that of Fe being 29.5 mm. The powders were mixed according to the Turbula principle at 30 revolutions per minute for 30 min and confirmed by energy dispersive X-ray analysis to achieve homogeneity [57]. Feedstock processing and electrical core and conductive winding was created using FDM; however, the relative permeability of the feedstock was low [52,111–113].

2.3. Fe–Co alloys

Interest in iron-based and cobalt-based amorphous alloys began in mid-1970s. In 1988, researchers at Hitachi included Nb and Cu additives for the production of amorphous alloys made from Fe or Co crystallites on the order of 10 nanometers (nm) in diameter. The presence of isolated transition metal crystallites reduced the eddy current losses greatly when compared with regular amorphous alloys [46]. Iron-cobalt alloys are known to have the highest maximum saturation magnetization (2.43 T at room temperature for a 35% Co and 65% Fe alloy) and Curie temperature among soft magnetic materials. They are unsurpassed in terms of high magnetic moments and high Curie temperature applications but are significantly more costly [13,114,115]; hence, they are mostly used for specialty applications and volume-constrained applications such as aerospace where the lighter weight compensates for the higher price. With a larger maximum flux density among soft magnetic families, Fe–Co alloys allow for electric machine designs that can be significantly reduced in size and weight. They are commercially available in various forms [116]. Permendur [117], supermendur [49], and Hiperco [64] are the most popular formulations, with the composition very close (49% Fe-49% Co–2% V). The mechanical strength, iron losses, and magnetic permeability can be controlled by varying the ratio between the cobalt and iron content, additional alloying of the material, or changing the temperature cycle during the annealing process.

Ternary or even quaternary phases of soft magnetic families with elements such as V, Mo, Nb, W, Ni, Ti, Mn, Cr, C, B, Zr, and Cu are alloyed to optimize the magnetic properties and corrosion resistance. Metals like V, Nb, and Ta are added to increase the ductility for the cold rolling of the alloys [114]. Co-based soft magnetic materials are key components of high temperature and high magnetization requirements [114,115]. Despite their superior magnetic properties, Co-based soft magnetic materials are very selectively applied because of the high price of Co. They are specifically used in high-efficiency electrical motors and Li-ion batteries [118]. There are a few examples of the AM of Fe–Co–based soft magnetic alloys [15,64,65,119,120]. Recently, Babuska et al. reported an SLM-manufactured, ductile, Fe–50Co binary alloy with a 250%–300% increase in yield strength and about an order of magnitude increase in ductility even without the addition of V [16]. They suggested a large improvement in the mechanical properties with the unique multiscale microstructures found in LENS additively manufactured samples. Kustas et al. demonstrated the LENS manufacturability of a Hiperco equivalent alloy [64]. The magnetic properties of the printed material were comparable to those obtained from conventional powder metallurgy. They used gas-atomized, prealloyed Fe–Co-1.5V powder as a printing precursor and built a thick-walled (~21 mm ID x 24.9 mm OD) and a thin-walled concentric cylinder 20 mm in height and studied their microstructures and magnetic properties. Fine equiaxed columnar grained microstructures were observed in LENS-manufactured samples, which transformed to a heterogenous, bimodal, grained structure after annealing at 1,111 K for 2 h. In another study, Kustas et al. verified that the suppression of the chemically ordered B_2 phase was possible by controlling the cooling rate during manufacturing [65]. Yang et al. reported the soft magnetic properties of $(Fe_{60}Co_{35}Ni_5)_{78}Si_6B_{12}Cu_1Mo_3$ [121] and SLM printing of $(Fe_{60}Co_{35}Ni_5)_{73.5}Si_{13.5}B_9CuMo_3$ alloys [119]. These alloys exhibited columnar microstructures along with dendrites of the a-Fe-(Co,Ni,Si) phase. The higher diffusion rate of Mo and B led to the formation of anisotropic Fe_3B phase, which increased the Fe–Si phase and saturation magnetization [121]. To control the grain size and improve the quality of the printed layers, they used laser remelting on $(Fe_{60}Co_{35}Ni_5)_{73.5}Si_{13.5}B_9CuMo_3$ [119] that exhibited body center cubic structure dominated microstructures. In a slightly different chemical composition, the impurity phase Fe_2B was recrystallized in the remelting process, and better soft magnetic properties (lower coercivity and higher saturation magnetization) were developed. Geng et al. synthesized high-throughput $Fe_{1-x}Co_x$ bulk samples using LENS and studied their structural and magnetic properties [120]. The Curie temperature, saturation magnetization, and magnetocrystalline anisotropy were functions of the Co concentration. Their study identified $Fe_{63}Co_{37}$ as a high saturation alloy that was comparable to previously reported bulk samples [83].

2.4. Soft magnetic composites

SMCs are insulation-coated magnetic particles that are often consolidated using high pressure to form a desired geometrical shape. They have been considered potential candidates since early 1990 [71]. The SMC refers to amorphous soft magnets, consolidated amorphous ribbon, and powder-based magnets and magnetic wires [122]. To date, SMCs are the main ingredients that allow fabrication of near-net shaped electrical cores in conventional manufacturing methods [123]. The isotropic distribution of magnetic particles in soft magnetic electrical cores produces ripple-free mechanical torque. The insulation coating increases the electrical resistance of the laminates, which is responsible for reducing losses from eddy currents; however, it greatly reduces the magnetization and mechanical strength of the electrical parts. In addition to

Table 5
Comparison of different approaches of manufacturing iron core, adapted and modified from Refs. [32,62].

Material families	Density (g/cm^3)	Tensile strength (N/mm^2)	Maximum permeability	Saturation flux density (T)	Core losses (W/kg)	Suggested applications	
						Flux path	Structure
Si steel sheet (e.g. M235-35A)	7.6	532	6,800	2.1	0.95 (50 Hz, 1 T) 69.8 (1 kHz, 1 T)	2D	2D
LOM-based laminated core	Similar mechanical, thermal, and electromagnetic properties like conventional Si steel sheet lamination					2D	Simple 3D
BJT-based core (Fe-6.5Si)	7.31	442.8	10,700	1.83	14.99 (60 Hz 1 T)	2D	2D
SMC (e.g. Hoganas 3P Somaloy700HR)	7.51	120	760	1.9	4.53 (50 Hz, 1 T) 137 (1 kHz, 1 T)	3D	3D
SLM-based iron core	Highest mechanical strength and thermal conductivity; Unable to suppress eddy current losses				High eddy current loss	–	3D

insulation, the compressed particles enclose air gaps, which greatly increases the resistivity. The SMCs should be produced either from iron or high-magnetic materials such as Fe_3P, Fe—Si, and Fe—Co alloys [46]. A benefit of AM with SMCs will be the achievement of more complex geometries than possible conventionally. FINEMET [68] is a Fe—Si rich SMC alloy (with a body-centered cubic Fe structure) that can be synthesized in fine-grained nanocrystalline forms with the addition of Cu, Nb, and B, yielding excellent soft magnetic properties. It can have moderate magnetization, extremely high permeability (40,000 to 100,000), and significantly high electrical resistivity. The use of AM has been reported for FINEMET [39,67,72,120,124,125]. It is also reported to be additively manufactured through SPS and LENS, with the latter producing soft magnets with coercivities of 1,194 to 3,024 A per meter.

2.5. Soft ferrites

Soft magnetic ferrites are cubic spinel structures with low coercivity ceramics formed by alloying Ni—Zn, Mn—Zn, or Co—Zn with magnetite (Fe_3O_4) [97]. They were reported as promising soft magnetic material with high resistivities in late 1940s [126]. Because of their higher resistivity, ferrites are very useful in high-frequency electrical components such as transformer cores and inductive toroidal cores in antenna [46]. Modern Mn—Zn ferrites can have magnetic permeabilities ranging from 350 to 20,000, whereas Ni—Zn ferrites can have permeabilities ranging from 15 to 2,000 [127]. Mn—Zn ferrites can have effective frequency ranges from 10 kHz to 10 MHz, whereas Ni—Zn ferrites can have effective frequency ranges from 1 to 100 MHz [50,128]. Although soft ferrites are not directly employed in rotating electrical machines, they are very promising feedstock materials for future multi-material AM processes to generate SMCs with low eddy current losses.

3. Survey of AM methods for electrical machines

From the literature survey, SLM, FDM, BJT, and LOM have been identified as potential AM methods for fabricating electric machines. In the section below, we discuss these methods including the process details, manufacturability, and scalability. Our survey revealed several early-stage opportunities in AM for enabling high-performance electric machine designs with complex core geometries. One such design example is geometric optimization of electric cores in switch reluctance motors to maximize the reluctance torque, which can eliminate or reduce the requirement for critical high-performance PMs [22,32]. Table 5 shows the comparison of physical properties of soft magnetic cores manufactured from different techniques and their associated flux geometries. LOM steel competes with conventionally manufactured steel, whereas SLM cores suffer from significant core losses. The BJT offers lower eddy current losses with full sintered density; however, the parts suffer from ~20% linear contraction during postprocessing [62]. In addition to achieving the required magnetic, electrical, and mechanical properties, fabricating larger electrical parts is a challenge in AM of electrical machines.

SMC, soft magnetic composite; SLM, selective laser melting; BJT, binder jetting technology; LOM, laminated object manufacturing.

Table 6 below shows the current large 3D printing machines and their size and available print volume and dimensions. Regarding the need of large electrical machine printing, BJT, SLM, LENS, and FDM or their combination looks appropriate approaches for the electrical machines printing.

Table 6
Current large 3D printers [129].

Printing technology	Printer name	Company	Build volume	Build dimensions	Availability
Binder Jetting	D-shape	Monolite UK	Infinite	–	Research
BJT	Voxeljet VX4000	Voxeljet	280 ft^3 (8.0 m^3)	3 × 6.6 × 3.3 ft (4.0 × 2.0 × 1.0 m)	Commercial
FDM	Infinite-Build	Stratasys	Infinite	–	Demonstrator
Concrete deposition	Winsun	Winsun	86,000 ft^3 (2,400 m^3)	130 × 33 × 20 ft (40 × 10 × 6.0 m)	Service
Concrete deposition	BetAbram P1	BetAbram	13,000 ft^3 (370 m^3)	52 × 30 × 8.2 ft (16 × 8.2 × 2.5 m)	Commercial
Deposition	BigDeltaWASP 12m	WASP	13,000 ft^3 (370 m^3)	20ø 40h ft (6ø 12h m)	Service
Concrete deposition	Imprimere 2156	Imprimere	8,000 ft^3 (230 m^3)	19 × 20 × 21 ft (5.8 × 6.0 × 6.3 m)	Commercial
FDM	BAAM	Cincinnati Inc.	900 ft^3 (25 m^3)	20 × 7.5 × 6.0 ft (6.1 × 2.3 × 1.8 m)	Service
FDM	ErectorBot 2076 LX	ErectorBot	840 ft^3 (24 m^3)	20 × 7.0 × 6.0 ft (6.1 × 2.1 × 1.8 m)	Commercial
FDM	KamerMaker	DUS Architects	480 ft^3 (14 m^3)	6.6 × 6.6 × 11 ft (2.0 × 2.0 × 3.5 m)	Demonstrator
EBAM	Sciaky EBAM 300	Sciaky	300 ft^3 (8.5 m^3)	19 × 4.0 × 4.0 ft (5.8 × 1.2 × 1.2 m)	Commercial
Laser Deposition	Mille HD	Millebot	200 ft^3 (5.7 m^3)	5.0 × 10 × 4.0 ft (1.5 × 3.0 × 1.2 m)	Commercial
Laser Deposition	RPM Innovations 557	RPM Innovations	180 ft^3 (5.0 m^3)	5.0 × 5.0 × 7.0 ft (1.5 × 1.5 × 2.1 m)	Service
FDM	3D Platform Excel	3D Platform	130 ft^3 (3.7 m^3)	4.0 × 4.0 × 8.0 ft (1.2 × 1.2 × 2.4 m)	Commercial
GDP	MASSIVit 1800	MASSIVit 3D	110 ft^3 (3.1 m^3)	5.9 × 4.9 × 3.9 ft (1.8 × 1.5 × 1.2 m)	Commercial
Fused Granular Fabrication (FGF)	The Box	BLB Industries	ft^3 (2.4 m^3)	4.9 × 3.6 × 4.9 ft (1.5 × 1.1 × 1.5 m)	Commercial
Ultrasonic Additive Manufacturing (UAM)	SonicLayer 7200	Fabrisonic	75 ft^3 (2.1 m^3)	5.0 × 5.0 × 3.0 ft (1.5 × 1.5 × 0.91 m)	Commercial
BJT	ExOne Exerial	ExOne	56 ft^3 (1.6 m^3)	7.2 × 3.9 × 2.0 ft (2.2 × 1.2 × 0.60 m)	Commercial
FDM	Tractus3D T3500	Tractus3D	53 ft^3 (1.5 m^3)	3.3ø 6.2h ft (1.0ø 2.0h m)	Commercial
FDM	The Atlas	Titan Robotics	49 ft^3 (1.4 m^3)	3.5 × 3.5 × 4.0 ft (1.1 × 1.1 × 1.2 m)	Commercial
LENS	Optomec LENS 850-R	Optomec	44 ft^3 (1.2 m^3)	3.0 × 4.9 × 3.0 ft (0.9 × 1.5 × 0.9 m)	Commercial
FDM	CoLiDo Mega	CoLiDo	42 ft^3 (1.2 m^3)	3.3ø 4.9h ft (1.0ø 1.5h m)	Commercial
SLA	The Mammoth	Materialise	41 ft^3 (1.2 m^3)	6.9 × 2.3 × 2.6 ft (2.1 × 0.70 × 0.80 m)	Service
FDM	BigRep ONE	BigRep	36 ft^3 (1.0 m^3)	3.3 × 3.3 × 3.3 ft (1.0 × 1.0 × 1.0 m)	Commercial
FDM	Cheetah	Fouche 3D Printing	36 ft^3 (1.0 m^3)	3.3 × 3.3 × 3.3 ft (1.0 × 1.0 × 1.0 m)	Commercial
FDM	Moebyus Machines M3	Moebyus Machines	36 ft^3 (1.0 m^3)	3.3 × 3.3 × 3.3 ft (1.0 × 1.0 × 1.0 m)	Commercial
FDM	HORI Z1000	Beijing Huitianwei Technology (HORI)	36 ft^3 (1.0 m^3)	3.3 × 3.3 × 3.3 ft (1.0 × 1.0 × 1.0 m)	Commercial
FDM	DeltaWASP 3MT	WASP	33 ft^3 (0.93 m^3)	3.3ø 3.9h ft (1.0ø 1.2h m)	Commercial
FDM	Builder Extreme 2000	Builder 3D Printers	32 ft^3 (0.91 m^3)	2.3 × 2.3 × 6.0 ft (0.70 × 0.70 × 1.8 m)	Commercial
SLM	The Aeroswift	Aerosud	26 ft^3 (0.74 m^3)	6.6 × 2.0 × 2.0 ft (2.0 × 0.60 × 0.60 m)	Service
FDM	Leapfrog XceL	Leapfrog	23 ft^3 (0.65 m^3)	1.8 × 1.7 × 7.6 ft (0.54 × 0.52 × 2.3 m)	Commercial
FDM	Fortus 900mc	Stratasys	18 ft^3 (0.51 m^3)	3.0 × 2.0 × 3.0 ft (0.91 × 0.61 × 0.91 m)	Commercial
FDM	I3D Innovation Multi512	I3D Innovation	18 ft^3 (0.51 m^3)	2.6 × 2.6 × 2.6 ft (0.80 × 0.80 × 0.80 m)	Commercial
FDM	German RepRap X1000	German RepRap	18 ft^3 (0.51 m^3)	3.3 × 2.7 × 2.0 ft (1.0 × 0.80 × 0.60 m)	Commercial
Rapid Plasma Deposition (RPD)	Merke IV	Norsk Titanium	6.0 ft^3 (0.17 m^3)	3.0 × 2.0 × 1.0 ft (0.91 × 0.61 × 0.30 m)	Service

FDM, fused deposition modeling; SLM, selective laser melting; BJT, binder jetting technology; EBAM, electron beam additive manufacturing; LENS, laser engineered net shaping; GDP, gel dispensed printing; SLD, stereolithography.

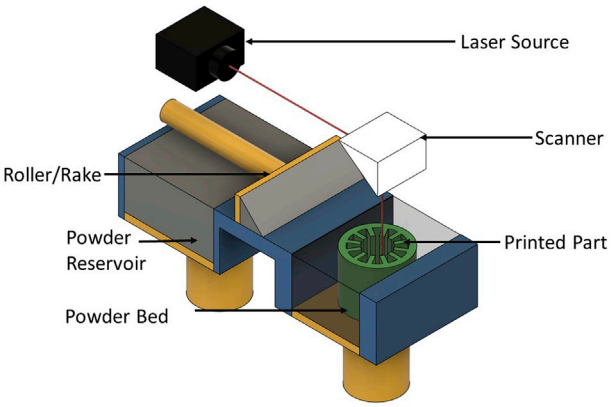

Fig. 7. Schematic of SLM printing of an electric stator core. SLM, selective laser melting.

For the suitability of production, these large machines often are of hybrid manufacturing nature. First, they print large parts, and the subtractive units maintains the surface finish and tolerances of the machines. There is no dedicated printer for large electrical machines yet. As the field will mature, more dedicated printer for large electrical machines will be developed. In the following sections, we will discuss a few research attempts on AM of electrical machines and highlight some of their main limitations.

3.1. Selective laser melting

Laser-based, layer-by-layer sintering AM technology is the most frequently used technology in metal AM. This method involves the use of a high-power laser to fully melt the alloy powder and fuse it layer-by-layer to produce the desired near net-shape with full density. Several researchers have demonstrated soft magnet processing using SLM [37,46,58–62,75]. In the SLM technology, the feedstock powder is spread over the fusion bed in a layer followed by melting using a laser beam as illustrated in Fig. 7. Then the sample bed is lowered, and another layer of the powder is spread and melted with a laser again until the full build is achieved. The key shape of the powder requirement for this process is spherical in nature [37,46,58–62,75]. This requirement could limit the use of certain alloy compositions.

Similar to SLM, LENS can provide rapid prototyping of experimental samples, especially convenient for metals and ceramics using a laser to generate the directed energy deposition melt [130]; however, it has limited capability to produce large electrical parts made from high-Si steel such as those used in wind turbine generators. So far, a few researchers have attempted designing and printing rotor cores for small-scale motors using SLM [7,51,56]; however, the printed steels have thus far exhibited lower quality. Fig. 8a–d shows examples of the SLM-printed rotor cores. The most common materials used in SLM-fabricated cores include Fe–Si and Fe–Co alloys. Tiismus et al. [30,131] highlight challenges associated with material processing of high-Si steel for motors using SLM, especially the formation of cracks and porosities, although a 50% mass reduction has been reported by optimizing the design with printed Fe-6.9Si for a 2-pole PM motor [32]. The fabricated material had higher specific power loss because of the solid core construction. While low ductility and poor thermal conductivity are also responsible for these defects, printing parameter optimization (e.g. energy input to powder bed), improvements in alloy composition and redesign can alleviate some of the effects caused by poor powder melting and porosities. Urbanek et al. [74] used SLM to additively manufacture the active rotor parts and the shaft for a surface-mounted PM motor. A post heat treatment was used to address anisotropy in mechanical properties, reduce residual stresses, and improve magnetic properties.

Researchers from VTT Research Center Finland [22] printed and designed a 6/4 pole switch reluctance motor with complex cavities using a Fe–Co alloy processed from SLM. The results demonstrated comparable magnetic saturation and mechanical properties with the standard Fe–Co alloy, although the specific power loss from eddy currents was high. Tseng et al. [31] proposed a novel rotor structure inspired by AM. They used SLM to fabricate an asymmetric rotor with a honeycomb structure that prevented flux leakage. They also experimentally validated the design that demonstrated a reduction in torque ripple by 45%. Neither research effort has progressed toward printing laminated sheets. There are also a few inherent challenges with SLM associated with sample quality. For example, SLM-prepared samples suffered from cracking and poor mechanical properties because of a large thermal gradient and defects such as porosity and incomplete fusion holes [133]. Additionally, the SLM technique will have issues with high vapor pressure elements such as magnesium, phosphorous, sulfur, zinc, and samarium. SLM could be a promising technique for achieving dense mechanical parts; however, careful selection of printing parameters would be necessary. The most influential printing parameters for SLM are laser power input, powder microstructure, hatching speed and space, annealing, preheating, and powder drying [8,14]. Also, the scanning pattern and scanning rates have a major influence on the finished part [32]. Moreover, managing a confined space to manufacture large machine parts will be a challenge. Laser melted feedstock materials and support structure oxidize immediately and need to protect under inert atmosphere which should cover both equipment and print area. Despite these challenges, larger SLM printers have been built in recent years. In 2016, the Wuhan National Laboratory for Optoelectronics manufactured one of the largest SLM printers at the time with a build volume up to 500 × 500 × 530 mm^3 [134]. Similarly, in 2017, Fraunhofer ILT acquired an 800 × 400 × 500 mm^3 build volume SLM printer [135]. However, these announced build volumes are still insufficient for large-scale multi-MW electric machines. A quick assessment of the importance of SLM including their advantages and disadvantages are listed in Table 7.

3.2. Fused deposition modeling

FDM is one of the most established AM processes that has been under the longest period of development and improvement among 3D printing technologies. In FDM, the low melting polymer or its composite is extruded on a printer bed in a layer-by-layer fashion as guided by a CAD model. A simple schematic of FDM printing is shown in Fig. 9. Molten polymer or polymer composite pellets have been used in the Big Area Additive Manufacturing (BAAM) facility [136]. Parts are built in a layer-by-layer fashion over the slightly heated bed. The temperature gradient helps to hold the part in place during printing. The details of the process and control strategies can be found in FDM-based literature on the AM of soft magnetic materials [77,87,94].

Peng et al. [73] printed and characterized ferrite-based soft magnets ($NiFe_2O_4$) with unique 3D structures using an extrusion free-forming technique coupled with a high-temperature, solid-state reaction process. The printed specimens demonstrated good magnetic properties; however, they suffered from drying cracks, requiring meticulous control over the drying rate. In an effort to achieve high power density aviation class motors, NASA [39] is pursuing efforts to FDM print soft magnets to realize complex stator geometries. Efforts to design and print a motor using an extrusion technique have also been reported by a team of

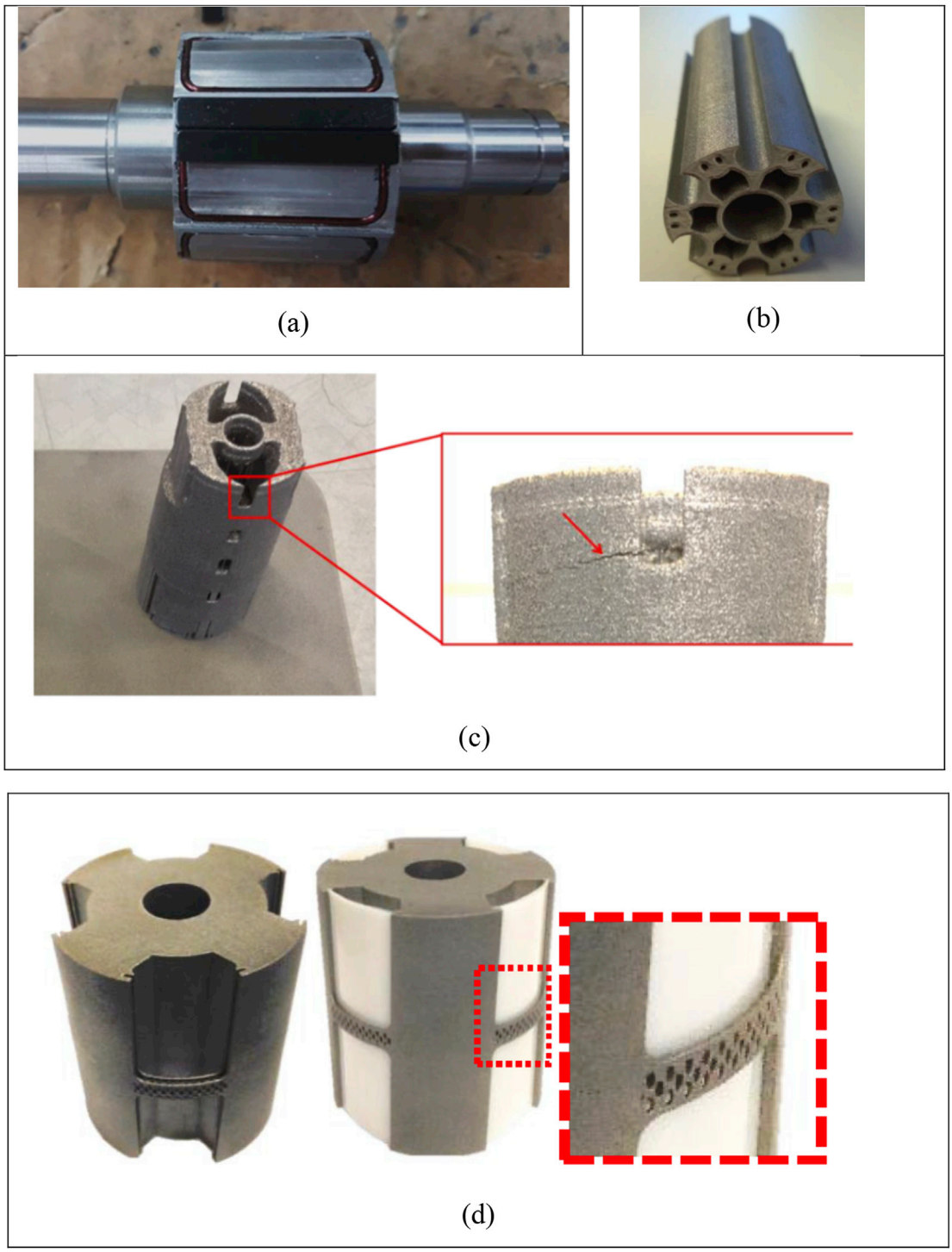

Fig. 8. (a) AM rotor active part and shaft of a PM motor [74] (permission granted for reprinting).; (b) a Fe–Co rotor core of a switch reluctance machine manufactured by SLM [22] (permission granted for reprinting).; (c) Fe-6.9Si rotor core for a 1-kW motor with a crack developed during printing enlarged at the right [132]; and (d) a novel skew rotor with honeycomb structure flux trap (enlarged in middle and right figures) realized by SLM [31]. (permission granted for reprinting). AM, additive manufacturing; PM, permanent magnet; SLM, selective laser melting.

researchers from Chemnitz University of Technology [137] as shown in Fig. 10. They designed a fully additively manufactured 6/4 pole switched reluctance machine for a flywheel system by multimaterial printing of the iron core, windings, and insulation. The printing process involved the use of pastes, extruded as in FDM printing, which were subsequently sintered together as in selective laser sintering techniques [85]. These pastes were composed of ceramic and metallic materials like copper and iron.

The FDM process requires relatively easier printing conditions. It can process diverse kinds of materials ranging from pure polymers to metal composites that can form a fused slurry. It can print large-volume artifacts because the print volume does not strictly require an inert atmosphere. Oak Ridge National Laboratory (ORNL) has printed both turbine blade molds and the blades themselves using the BAAM FDM printer in the Manufacturing Demonstration Facility [138]. ORNL and Ingersoll Machines Tools Inc. have also

Table 7
Advantages and disadvantages of SLM.

S. No.	Advantages	Disadvantages
1	Can fabricate dense parts with high saturation magnetization	Defects are inherent e.g. melt pools, porosity, internal stress, and unreacted powder spot
2	Can print diverse kind of metals and polymers	Very slow process in comparison to BJT and FDM
3	Mechanically strong parts	Relatively high eddy current loss in electrical cores
4	No significant post processing is required	Machinery can be expensive (not as expensive as e-beam)
5	No support is necessary. However, print plate is necessary	Requires strict safety and maintenance
6	No contaminating medium are required	Printed part removal is rather difficult
7		High power consumption

FDM, fused deposition modeling; SLM, selective laser melting; BJT, binder jetting technology.

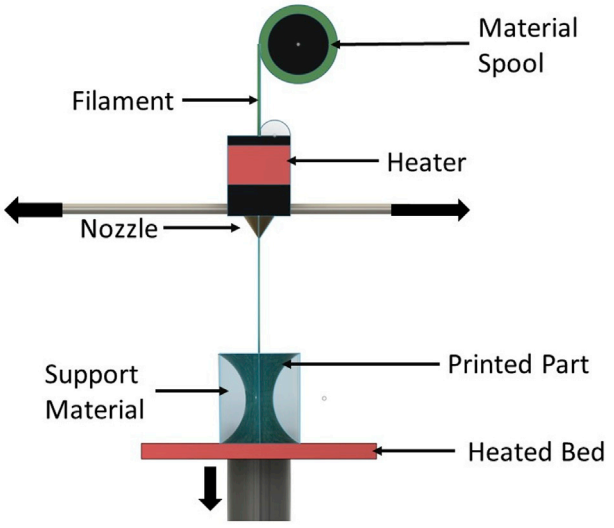

Fig. 9. Schematic of FDM printing. FDM, fused deposition modeling.

partnered to develop the Wide and High Additive Manufacturing system with one of the largest FDM print volumes in the United States (W 23 feet x H 10 feet x L 46 feet) [139]. The University of Maine is also reported to have printed the world's largest 3D-printed boat (7.62 m long and weighing 2.2 tons) [140]. The same team is also planning to print a 23-meter-long bridge girder [140]. This progress in large parts printing using FDM is encouraging for the next generation of manufacturing industries. The major challenge in the electrical machines FDM technology is the decrease in specific power because of lower fraction of loaded magnetic particles and subsequent decrease in mechanical properties; however, the eddy current loss is greatly reduced because of its higher electrical resistivity. The advantages and disadvantages of the FDM method are presented in Table 8.

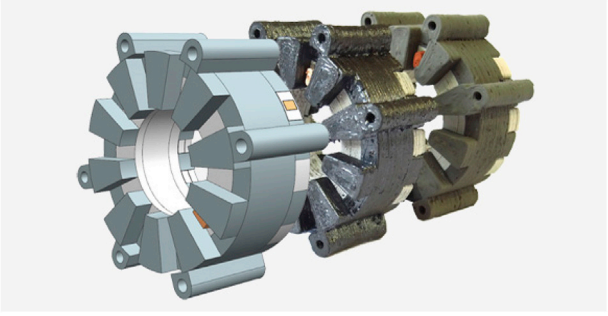

Fig. 10. Chemnitz University of Technology's stator for a winding-less reluctance machine produced by extrusion technique showing the CAD design, printed green part, and postheat-treated product. (courtesy: J. Rudolph) [137]. (For interpretation of the references to color in this figure legend, the reader is referred to the Web version of this article.). CAD, computer-aided design.

3.3. Binder jet technology

In BJT, feedstock layers are bound with the selective injection of binding liquid to acquire a desired shape of the printed parts, which is ultimately debound by heat treatment. This method can be used with both permanent binders and low melting metals or sacrificial

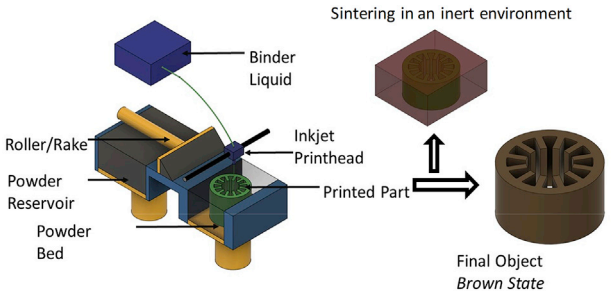

Fig. 11. Schematic of BJT of stator electrical core and heat treatment. BJT, binder jetting technology.

Table 8
Advantages and disadvantages of FDM.

S. No.	Advantages	Disadvantages
1	Can print any kind of magnetic materials	Saturation magnetization M_s is reduced because of non-magnetic polymer
2	Eddy current loss can be greatly reduced with high resistivity of polymers	Thermal conductivity is reduced
3	Low temperature processing is useful to preserve the magnetic properties during printing	Mechanical properties are poor especially in build direction
4	Improved corrosion resistance	Frequent nozzle clogging
5	Low lead time and production cost	Limited to thermoplastic polymers
6	Large parts production is possible	
7	Machinery easy and safe to operate	
8	Multimaterial printing is possible	

FDM, fused deposition modeling.

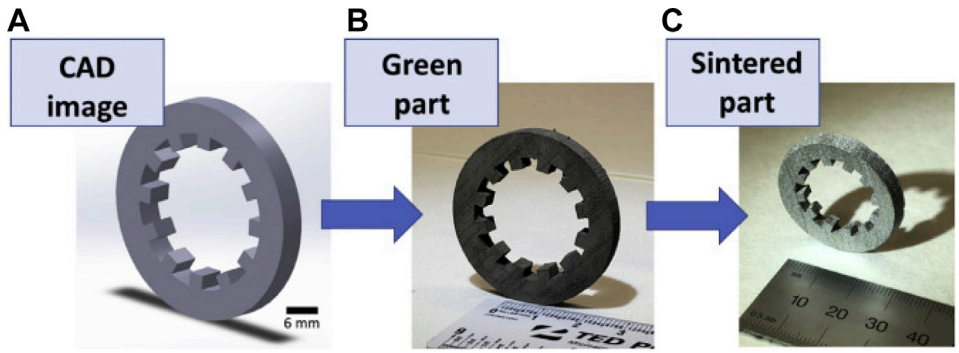

Fig. 12. (a) CAD image; (b) printed Fe-6.5Si green part; and (c) sintered stator core using BJT [62]. (For interpretation of the references to color in this figure legend, the reader is referred to the Web version of this article.) CAD, computer-aided design; BJT, binder jetting technology.

Table 9
Advantages and disadvantages of BJT.

S. No.	Advantages	Disadvantages
1	Relatively difficult but large parts can be fabricated	Needs extensive postprocessing
2	Can print both metals and ceramics	Porosity and sacrificed carbon remain in the material that degrades magnetic property
3	Provides freedom of debound or injecting additional material post printing	Infiltration is required for better mechanical properties in most of the cases
4	Can process all kinds of powders	Tolerance maintenance is a great problem
5	No support structure is required	
6	Cheaper to fabricate parts than e-beam and SLM	

SLM, selective laser melting; BJT, binder jetting technology.

binders that can be debound and ultimately achieve full density through a solid-state sintering process. A schematic of the BJT process for a stator core is shown in Fig. 11. BJT resembles a metal injection molding process [86] and it can provide an opportunity with liquid infiltration to significantly tune the desired material properties. It can process diverse materials including soft magnetic metal powders, ceramics, and polymers [62,96,141]. Cramer et al. [55] demonstrated a novel method to fabricate a near-net shape, fully dense soft magnetic Fe-6.5Si stator ring through BJT, followed by solid-state sintering to mitigate cracking. The printed Fe-6.5Si parts showed several advantages, such as a reduction in core loss at low, medium, and high frequencies, high resistivity, and good magnetic permeability. The study also suggests the possibility of tuning the permeability, either by increasing the grain size or reducing the thickness of the stator ring. This was also the first study that proposed slicing to obtain thinner parts from printed rings.

Fig. 12a–c shows the sequence of the BJT manufactured Fe-6.5Si alloy (PSD067, d90 < 22 μm) stator ring CAD model, green part, and sintered printed part using the ExOne Lab big area binder jet machine. The alloy powder was used with ProMetal R-1 ExOne's proprietary commercial binder material to obtain the as-printed green part. The printed green parts were air dried at 200°C for 1 h and debinding was carried out by heat treatment for 1 h at both 630°C and 900°C under an argon atmosphere flowing at a rate of 300 cubic centimeters per minute [62]. Finally, the debound parts were sintered at 1,300°C for 2 h under 10^{-5} Torr vacuum. The sintered part shrank linearly in all directions; we know that up to 20% linear contraction can occur in the sintered part. It is possible that the designed dimensions of electric parts may need to be overestimated by a certain factor, followed by machining at the end to maintain the tolerance.

Researchers from Michigan State University have successfully applied BJT to print high-Si steel with high permeability [75]. It is perceived that the absence of thermal gradient during heat treatment can result in less cracking and lower thermal stresses. BJT also makes the printing of complex geometries possible that are otherwise impossible using molding and sintering. It can be a good candidate for large electrical parts printing. One of the largest available volumes for BJT is provided by the VX1000 by Voxeljet (build space up to 2,000 × 1,000 × 1,000 mm^3) [142]. However, identifying an appropriate binder that does not degrade the quality of feedstock materials and that can be comfortably debound is always a great challenge. BJT can allow larger realizable print volumes; but similar to FDM, there could be challenges in postprocessing the printed parts. The advantages and disadvantages of the BJT are listed in Table 9.

3.4. Laminated object manufacturing

The LOM method resembles hybrid printing because it includes both layer addition and extensive cutting and machining. It also closely resembles conventional electrical machine production. One of the least practiced AM methods despite its close resemblance

Table 10
Advantages and disadvantages of LOM.

S. No.	Advantages	Disadvantages
1	Fast paced processing	Energy demanding processing including cutting, machining, and welding
2	No or very little post processing	Limited stacked type topologies are possible
3	Waste is mostly recycled	Limited processing materials are available
4	No need for support structure	
5	Produces robust and rugged electrical parts	

LOM, laminated object manufacturing.

with conventional electrical core production using soft magnetic material processing and electrical machine production is LOM. Because the stator and rotor cores of electrical machines typically consist of a stack of thin laminated insulation coated sheets, AM can effectively print the sheet of desired thickness and either coat with insulation ex-situ or even in-situ through multimaterial printing. For example, Feygin et al. patented the LOM technique to facilitate the automated AM of 3D objects using geometrical models and laminates [143,144]. Wu and El-Refaie recently outlined simple steps to fabricate the iron core using the LOM technique [32]. This LOM method could be beneficial to produce low-thickness laminated sheets for high-Si steel and Fe—Co—V alloy, overcoming their low workability. Although this method could impact electrical machine production, there are very few and loosely related LOM techniques dedicated to electric machines. The Best Electric Machine MOTORPRINTER [145] is the only known industrial printer for the rapid commercial AM of electric machine cores with high-performance electrical steel, such as amorphous metal ribbon, using sheet lamination 3D printing technology. It is perceived, however, that sheet lamination 3D printing may be limited by the smallest adhesive thickness, which is important for iron loss reduction as well as stacking factor control [36]. The advantages and disadvantages of this method are presented in Table 10.

4. Outlook

An acceptable manufacturing model for the 21st century supports persistent economic growth as well as the sustainability of natural resources and the environment. It should be able to address the demand for efficient and portable electrical machines, waste reduction, and economical uses of critical materials. The next level of sophistication in the manufacturing industry is possible if AM of magnetic materials and their integration in electrical machine is possible. There is deep interest among researchers and machine manufacturers to produce the most advanced, high power dense, electric machine of almost any shape, size, and high-performance materials directly from their 3D CAD models. However, attempts to turn powders of advanced materials into functional electrical machines with reduced printing operations, simpler postprocessing steps, and consequently fewer number of parts to assemble is still in early stages.

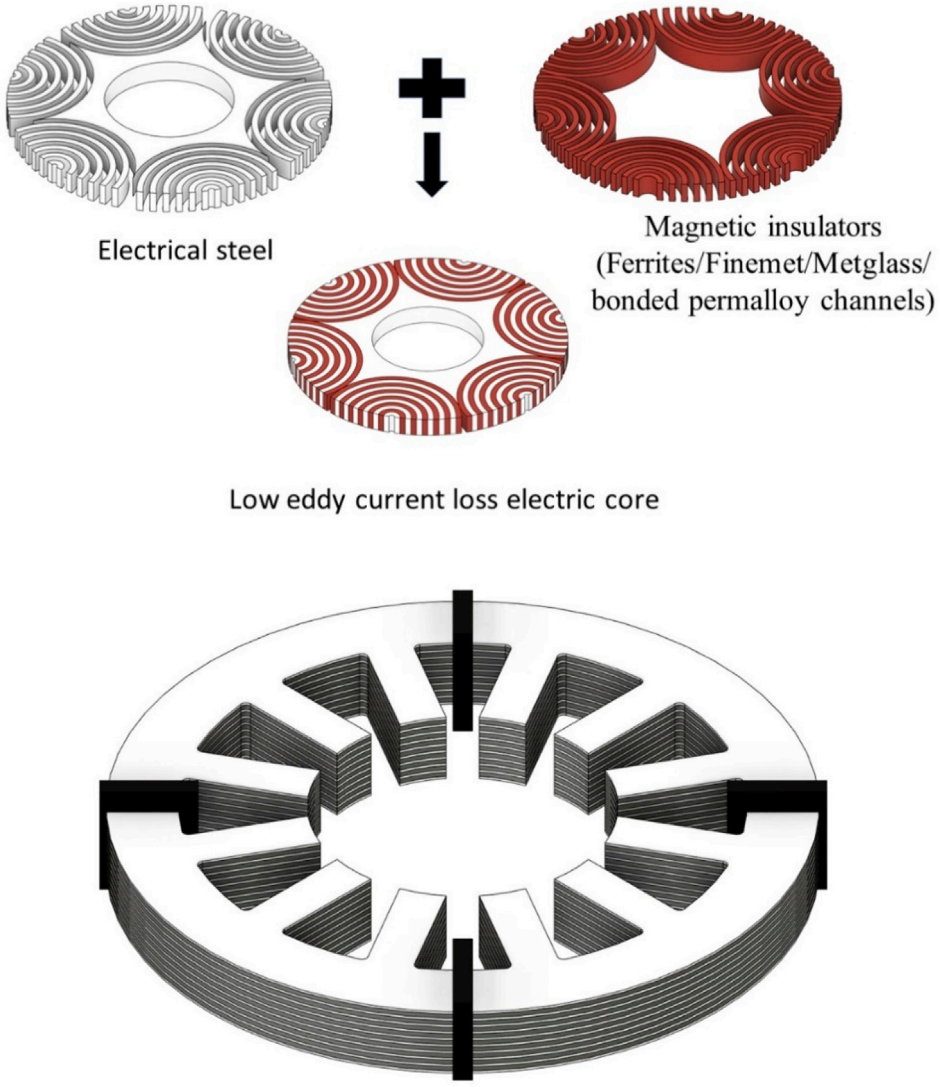

Fig. 13. Low eddy current loss synchronous electrical core design with alternating thin vertical cylindrical sheets of steel and magnetic insulator (top) and horizontal stacking (bottom). Yoke and clamps can be introduced to reinforce the mechanical strength.

Apart from improving the current state of the art of conventional manufacturing of electrical machines, the next level of sophistication in electric machine manufacturing can be realized if multimaterial AM of magnetic materials and their integration into the electric machine becomes possible. Currently, uncertainties in the delivery form (processed, semi-processed), the relatively slow manufacturing speed, internal defects from layer-by-layer fabrication, limited multimaterial capabilities, and necessary post-production of printed parts are major limitations in achieving this goal. Next, we will briefly discuss the potential criteria that must be satisfied before the AM of magnetic materials for electric machines can be commercialized.

4.1. Increasing the quality and workability of feedstock materials

AM can facilitate improvements in the quality of feedstock materials as well as the final product. For example, Fe−3Si is the key component of most electric machines because of its ductility for cold rolling despite its larger eddy current loss because of larger magnetostriction and lower permeability when compared with Fe-6.5Si [104]. However, AM can enable routes for Fe-6.5Si processing, such as SLM of already prepared powder from a viable route such as rapid solidification process [101] followed by mechanical ball-milling and sieving for feedstock microstructure sizes control. Also, the print direction and laser power can control the grain orientation in Fe-6.5Si build parts that are not easily available in conventional powder processing. Additionally, BJT can avoid the defects associated with cracks and porosity formation both in cold rolling as well as SLM. BJT can fulfill the printing of reasonably large machine parts by allowing the postprocessing freedom only for the printed parts without necessitating the protective environment for the whole printer assembly as in the SLM method.

4.2. Use of computational tools in design prediction, operation, and maintenance of electrical machines and power supplies

The capability of AM to print complex parts and reduce their count by replacing the sets of complex arrays of mechanical parts with a specified functional part can be assisted by predicting the optimal geometries and strength [146] using modern computational tools thereby reducing cost and weight of the machine. One industry that provides great examples of the benefits of AM is aerospace. In traditional manufacturing techniques, components such as engines have typical buy-to-fly ratios of 4:1, meaning that the total weight of the raw materials is four times than the weight of the finished component. General Electric's redesigned LEAP engine, which has AM nozzles that increase the engine efficiency, demonstrated higher durability and weighed 25% less than a conventionally manufactured jet engine. The AM process also simplified the design by reducing the number of components from 20 welded pieces to one [3]. These benefits can be transferred to electrical machines. With the assistance of topology optimization software, the most efficient geometries for the magnets and core can be achieved. Such geometries can be realized through AM, thus creating significantly lighter electric parts.

In addition to topology optimization, certain advanced computational techniques including the use of ML and finite element analysis can help in 3D printing process monitoring [26], energy production and consumption modeling [147], cyber-attack prevention in power grids, and prediction of machine failures [148]. Computational tools could also be beneficial in prediction of optimal processing parameters. Laser scanning patterns using island and helical strategies have been used to alleviate defects and internal stress in the material of interest [149]. These tools could predict an optimized scanning model for tailoring the physical properties of the materials. Additionally, such methods can aid the analyses of and real time processing of images and machine signals that can assist in early detection of problems both in printers and printed electrical machines. Relevant sensors could be designed and integrated in final printed parts for early detection of faults or timely maintenance. As grid penetration from wind power increases, electrical power supply will fluctuate more than ever. The supply chain system would require new level of fault detection, tolerance, and maintenance system [150−152]. Digital control system will allow analysis and prediction of fault trends and printing process and machine operations failures. More importantly, large electrical offshore machines need to be installed far away from regular security services, and they are vulnerable to cyber-attack to disrupt their operation and performances. AI-based novel false data injection attacks prediction and detection systems are proposed to maintain the security of the powder feeding lines [148].

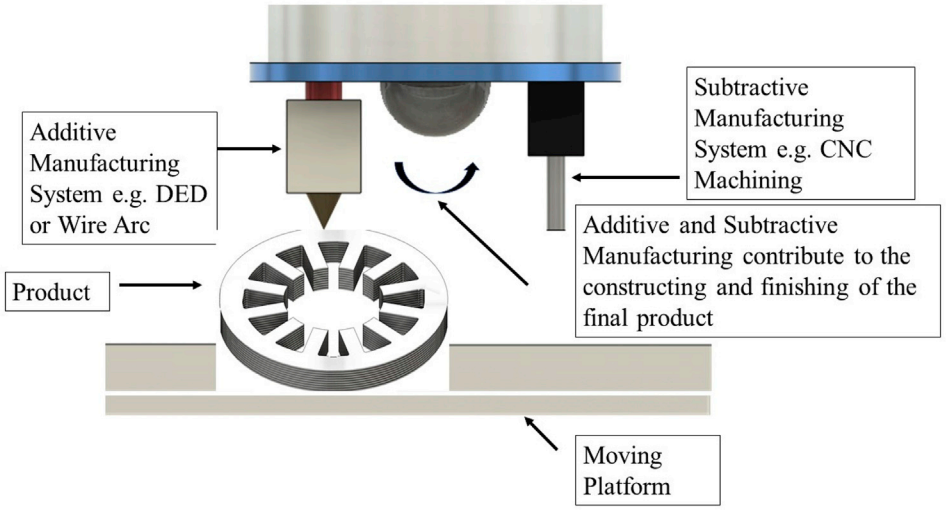

Fig. 14. A schematic of hybrid manufacturing for electrical stator core which includes combination of AM methods and CNC lathe machines. AM, additive manufacturing; CNC, computerized numerical control; DED, directed energy deposition.

4.3. Designing multimaterial processing technologies and machineries

Electrical machines can include PMs, a soft magnetic stator and rotor, electrical windings, insulation, a heat exchanger, and mechanical support structures. The goal for the manufacturing industry will be to develop a single-step end-use product printing process with an optimum price. One of the methods that can change the paradigm of the electrical core is direct printing of electrical cores either with alternate concentric vertical sheets of high-Si steel and magnetic insulators (e.g. soft ferrites) or alternate stacking layers as shown in Fig. 13 [76]. One significant challenge will be the design of a stable interface between the electrical steel and magnetic insulators. Such a design might suffer from mechanical properties, which could be overcome with steel yokes and pegs of appropriate types. This method will overcome the issue with magnetization reduction with insulation and significantly increase the eddy current loss via high electrical resistance, and the specific power of the electrical core could surpass traditional laminated cores. There are some examples of multimaterial 3D-printed electrical machines already showing great promise, such as a magnetic soft actuator [99]. There are several ongoing multimaterials AM efforts in this area, including Manufacturing and Additive Design of an Electric Machine enabled by 3D printing led by NREL and ORNL, work by Chemnitz University of Technology [99], NRC [153], and more. In addition to multimaterial synchronous electric cores, hybrid synchronous reluctance electric cores can be easily realized by designing inserting slots [154]. All of these scenarios suggest a bright future for multimaterial AM of electric cores.

A successful multimaterial AM of electrical machines requires hybrid printing technologies. A hybrid printing incorporates combination of both additive methods for building the parts and subtractive methods such as computerized numerical control (CNC) lathes to maintain the surface finish and parts tolerance so that limitation on both methods are synergistically eliminated [155,156]. It also broadly refers to composites printing, implementing sequence of printing methods and materials dispensing schemes, real time closed-loop quality control mechanism, and postprocessing methods [157,158]. Fig. 14 shows a schematic of hybrid manufacturing setup for electrical stator for multimaterial printing. Eddy current loss is proportional to square of thickness of the core laminates which is a tough constraint that cannot be avoided for both subtractive and additive manufacturing. Instead of printing electrical cores and machining them, near net shape end-use printing of electrical core is possible if multiple materials can be deposited in desired order during layer fabrication. To realize the multimaterial core, material dispensing for the parts forming sequences are important. In the multimaterials printing of the large electrical machines will probably generate much larger powder waste with powder mixing as well as processing means contamination such as quality degradation with repeated exposure to laser, heat, and binder that ultimately forms a cake on the surface of the parts which is very difficult to recycle as well as machining. This can be avoided by introducing robotic arm to dispense the feedstock materials only on top of the printed part and collect back the surplus powder before laser activation and binder secretion. Another approach could be powder feedstock for electrical high Si steel and rod or bound fiber for the soft ferrite/magnetic insulators/amorphous materials so that different types of printing techniques can be switched between successive layers. A simple conceptual printers and CNC lathe machines arrangement is shown in Fig. 14. Here, the printing bed is accessible for multiple processing technique at a time and best method can be picked to dispense and fabricate a layer. The central part of the large electrical core printing could generate a large waste of feedstock materials which could be avoided either by introducing disposable ceramics protective gear that synchronously responses to avoid the powder spreading in successive iteration. Finally, the printed parts are post processed properly and maintain the tolerance using subtractive machines such as CNC lathes accessed using the movable printing bed.

Regarding the multimaterials processing in hybrid printing of the electrical machines, another area of focus could be co-printing the unconventional winding for inductors using ultrahigh conductive carbon nanotube-copper composite wire to achieve the minimal winding losses [159,160]. 3D printed graphene loaded flexible electrical conductive fibers are already reported [161]. Similarly, there are several benefits and challenges of copper wire 3D printing are already known [162,163]. By improving the method of dispensing the axially aligned carbon nanotubes and graphene fibers along the axis of the wire, hybrid printing could contribute in manufacturing of low loss electrical windings.

5. Concluding remarks

As with the general trend of metal AM technologies, SLM, FDM, and BJT are the most popular methods for AM of soft magnetic materials for electrical machines. In addition, the list of potential soft magnetic materials suitable for AM has been identified. The progress in AM of soft magnetic materials and their integration in electrical machines is rapidly advancing. The need for large-scale printing of electric machines remains a key priority; for example, large-scale demonstrations are essential to realize the world's most advanced, lightweight, ultra-efficient electric machines with high torque density and little to no critical rare-earth PMs. Multimaterial AM is explicitly positioned to address the aforementioned challenges that are barriers to particularly large-scale wind generator manufacturing by advancing capabilities for the design and on-site AM of generator active (magnetic/electric) sections with little or no critical rare earth PMs and also inactive (structural) materials. This requirement justifies continued investment in the AM process of electric machines. To achieve the manufacturing maturity of large electrical machines, much robust hybrid printing protocols are desired.

Declaration of competing interest

The authors declare that they have no known competing financial interests or personal relationships that could have appeared to influence the work reported in this article.

Acknowledgments

The research was supported by the U.S. Department of Energy, Office of Energy Efficiency and Renewable Energy, Wind Energy Technologies Office Program. This manuscript has been jointly authored by UT-Battelle, LLC, under contract No. DE-AC05-00OR22725 with the US Department of Energy (DOE) and the National Renewable Energy Laboratory, operated by Alliance for Sustainable Energy, LLC, for the U.S. Department of Energy (DOE) under Contract No. DE-AC36-08GO28308.

The US government retains and the publisher, by accepting the article for publication, acknowledges that the US government retains a non-exclusive, paid-up, irrevocable, worldwide license to publish or reproduce the published form of this manuscript, or allow others to do so, for US government purposes. DOE will provide public access to these results of federally sponsored research in accordance with the DOE Public Access Plan (http://energy.gov/downloads/doe-public-access-plan).

Abbreviations

AM	Additive Manufacturing
BAAM	Big Area Additive Manufacturing
BJT	Binder Jetting Technology
H_c	Coercivity
CNC	Computerized numerical control
CS	Cold Spray
CAD	Computer-Aided Design
DLP	Digital Photolithography
DED	Directed Energy Deposition
P_{exc}	Domainwall Motion
P_{ec}	Eddy Current Losses
EBAM	Electron Beam Additive Manufacturing
EDM	Electrical Discharge Machining
r	Electrical Resistivity
FDM	Fused Deposition Modeling
FFF	Fused Filament Fabrication
FGF	Fused Granular Fabrication
P_{hyst}	Hysteresis
LOM	Laminated Object Manufacturing
LBM	Laser Beam Melting
LENS	Laser Engineered Net Shaping
L-PBF	Laser Powder Bed Fusion
lamda	Magnetostriction Parameter
MW	Megawatt
MAC	Mitsui Automatic Core assembly
NRC	National Research Council
ORNL	Oak Ridge National Laboratory
PM	Permanent Magnet
μ_r	Relative Permeability
B_r	Remanence
M_s	Saturation Magnetization
SLM	Selective Laser Melting
SMC	Soft Magnetic Composites
SPS	Spark Plasma Sintering
SLA	Stereolithography
3D	Three dimensional
TRL	Technology Readiness Level
k	Thermal Conductivity
WHAM	Wide and High Additive Manufacturing
UAM	Ultrasonic Additive Manufacturing

References

[1] A. El-Refaie, M. Osama, High specific power electrical machines: a system perspective, CES Trans. Electr. Mach. Syst. 3 (1) (Mar 2019) 88–93, https://doi.org/10.30941/CESTEMS.2019.00012.

[2] M. Henke, et al., Challenges and opportunities of very light high-performance electric drives for aviation, Energies 11 (2) (Feb 2018) 344, https://doi.org/10.3390/en11020344.

[3] M. Ghassemi, High power density technologies for large generators and motors for marine applications with focus on electrical insulation challenges, High Volt. 5 (1) (2020) 7–14, https://doi.org/10.1049/hve.2019.0055.

[4] Componentized Direct-Drive Electric Generator Targets New and Refurbished Wind Turbines, Oct 1 2019. Electronic Design, https://www.electronicdesign.com/power-management/article/21808641/componentized-directdrive-electric-generator-targets-new-and-refurbished-wind-turbines. (Accessed 10 March 2020).

[5] G.E. Fish, Soft magnetic materials, Proc. IEEE 78 (6) (Jun 1990) 947–972, https://doi.org/10.1109/5.56909.

[6] A. Krings, Iron Losses in Electrical Machines - Influence of Material Properties, Manufacturing Processes, and Inverter Operation, 2014.

[7] N. Urban, A. Meyer, M. Leckel, M. Leder, J. Franke, Additive manufacturing of an electric drive a feasability study, in: 2018 International Symposium on Power Electronics, Electrical Drives, Automation and Motion (SPEEDAM), Jun 2018, pp. 1327–1331, https://doi.org/10.1109/SPEEDAM.2018.8445258.

[8] J.-Y. Lai, A Study of the Fabrication of Thin Lamination Stator Cores by the Uniform Droplet Spray Process, Thesis, Massachusetts Institute of Technology, 1997.

[9] T. Wakisaka, Y. Kurosaki, S. Arai, Electrical Steel Sheet for Traction Motor of Hybrid/Electrical Vehicles, vol. 103, 2013, p. 5.

[10] Precision tooling/precision parts | PRODUCTS | Mitsui High-Tec, Inc. https://www.mitsui-high-tec.com/en/products/kg/ (accessed Apr. 18, 2020).

[11] J.-P. Kruth, M.C. Leu, T. Nakagawa, Progress in additive manufacturing and rapid prototyping, CIRP Ann. 47 (2) (Jan 1998) 525–540, https://doi.org/10.1016/S0007-8506(07)63240-5.

[12] S.A.M. Tofail, E.P. Koumoulos, A. Bandyopadhyay, S. Bose, L. O'Donoghue, C. Charitidis, Additive manufacturing: scientific and technological challenges, market uptake and opportunities, Mater. Today 21 (1) (Jan 2018) 22–37, https://doi.org/10.1016/j.mattod.2017.07.001.

[13] E. Atzeni, A. Salmi, Economics of additive manufacturing for end-useable metal parts, Int. J. Adv. Manuf. Technol. 62 (9) (Oct 2012) 1147–1155, https://doi.org/10.1007/s00170-011-3878-1.

[14] S. Yang, Y. Tang, Y.F. Zhao, A new part consolidation method to embrace the design freedom of additive manufacturing, J. Manuf. Process. 20 (Oct 2015) 444–449, https://doi.org/10.1016/j.jmapro.2015.06.024.

[15] D. Goll, et al., Additive manufacturing of soft magnetic materials and components, Addit. Manuf. 27 (May 2019) 428–439, https://doi.org/10.1016/j.addma.2019.02.021.

[16] T.F. Babuska, et al., Achieving high strength and ductility in traditionally brittle soft magnetic intermetallics via additive manufacturing, Acta Mater. 180 (Nov 2019) 149–157, https://doi.org/10.1016/j.actamat.2019.08.044.

[17] Process Steps in the Metal Additive Manufacturing Workflow, Dec 13 2018. Digital alloys, https://www.digitalalloys.com/blog/process-steps-metal-additive-manufacturing-workflow/. (Accessed 19 April 2020).

[18] 2018-05-23 Aya Bentur, "Additive Manufacturing Workflows - Infographics and More", May 23 2018. LEO Lane, http://www.leolane.com/blog/additive-manufacturing-workflows-infographics/. (Accessed 9 May 2020).

[19] K. Minet, A. Saharan, A. Loesser, N. Raitanen, 8 - superalloys, powders, process monitoring in additive manufacturing, in: F. Froes, R. Boyer (Eds.), Additive Manufacturing for the Aerospace Industry, Elsevier, 2019, pp. 163–185.

[20] TRUMPF Introduces Precious Metal and Copper 3D Printing Powered by Green Laser, Nov 20 2018, 3D Printing Industry, https://3dprintingindustry.com/news/trumpf-introduces-precious-metal-and-copper-3d-printing-powered-by-green-laser-143689/. (Accessed 5 May 2020).

[21] Y. Yan, Chao Ding, K.D.T. Ngo, Y. Mei, G.-Q. Lu, Additive manufacturing of planar inductor for Power Electronics applications, in: 2016 International Symposium on 3D Power Electronics Integration and Manufacturing (3D-PEIM), Jun 2016, pp. 1–16, https://doi.org/10.1109/3DPEIM.2016.7570536.

[22] Metsä-Kortelainen, Sini; Lindroos, Tomi; Savolainen, Mikko; Jokinen, Antero; Revuelta, Alejandro; Pasanen, Antti; Ruusuvuori, Kimmo; Pippuri, Jenni, Manufacturing of Topology Optimized Soft Magnetic Core Through 3D Printing; *VTT Technical Research Centre of Finland Ltd.*, Accessed: Mar. 14, 2020. [Online]. Available: https://www.vttresearch.com/Documents/Factory%20of%20the%20future/3D%20printing/2NAFEMS_2016_Finland_Fe-Co_rotors_Pippuri.pdf.

[23] C. Pompermaier, J. Washington, L. Sjöberg, Axial Flux PM Machines for Compressor Application, 2017, p. 4.

[24] Soft Magnetic Composites | Höganäs/en/powder-technologies/soft-magnetic-composites/ (accessed May 16 2020).

[25] J. Straub, Initial work on the characterization of additive manufacturing (3D printing) using software image analysis, Machines 3 (2) (Jun 2015) 55–71, https://doi.org/10.3390/machines3020055.

[26] U. Delli, S. Chang, Automated process monitoring in 3D printing using supervised machine learning, Procedia Manuf. 26 (Jan 2018) 865–870, https://doi.org/10.1016/j.promfg.2018.07.111.

[27] S. Nuchitprasitchai, M.C. Roggemann, J.M. Pearce, Three hundred and sixty degree real-time monitoring of 3-D printing using computer analysis of two camera views, J. Manuf. Mater. Process. 1 (1) (Sep 2017) 2, https://doi.org/10.3390/jmmp1010002.

[28] A. Krings, A. Boglietti, A. Cavagnino, S. Sprague, Soft magnetic material status and trends in electric machines, IEEE Trans. Ind. Electron. 64 (3) (2017) 2405–2414, https://doi.org/10.1109/TIE.2016.2613844.

[29] M. C. Halbig and M. Singh, "Enabling Additive Manufacturing Technologies for Advanced Aero Propulsion Materials & Components," p. 32.

[30] H. Tiismus, A. Kallaste, A. Belahcen, A. Rassölkin, T. Vaimann, Challenges of additive manufacturing of electrical machines,, in: 2019 IEEE 12th International Symposium on Diagnostics for Electrical Machines, Power Electronics and Drives (SDEMPED), Aug 2019, pp. 44–48, https://doi.org/10.1109/DEMPED.2019.8864850.

[31] G.-M. Tseng, K.-J. Jhong, M.-C. Tsai, P.-W. Huang, W.-H. Lee, Application of additive manufacturing for low torque ripple of 6/4 switched reluctance motor, in: 2016 19th International Conference on Electrical Machines and Systems (ICEMS), Nov 2016, pp. 1–4.

[32] F. Wu, A.M. El-Refaie, Towards fully additively-manufactured permanent magnet synchronous machines: opportunities and challenges, in: 2019 IEEE International Electric Machines & Drives Conference (IEMDC), May 2019, pp. 2225–2232, https://doi.org/10.1109/IEMDC.2019.8785210. San Diego, CA, USA.

[33] J.-M. Lamarre, F. Bernier, Permanent magnets produced by cold spray additive manufacturing for electric engines, J. Therm. Spray Technol. 28 (7) (Oct 2019) 1709–1717, https://doi.org/10.1007/s11666-019-00917-6.

[34] R. Wrobel, B. Mecrow, Additive manufacturing in construction of electrical machines – a review, in: 2019 IEEE Workshop on Electrical Machines Design, Control and Diagnosis (WEMDCD), vol. 1, Apr 2019, pp. 15–22, https://doi.org/10.1109/WEMDCD.2019.8887765.

[35] H. Tiismus, A. Kallaste, A. Rassölkin, T. Vaimann, Preliminary Analysis of Soft Magnetic Material Properties for Additive Manufacturing of Electrical Machines, 2019. Key Engineering Materials /KEM.799.270. (Accessed 6 March 2020).

[36] F. Bernier, M. Ibrahim, M. Mihai, Y. Thomas, and J.-M. Lamarre, "Additive Manufacturing of Soft and Hard Magnetics Materials Used in Electrical Machines," p. 16.

[37] N.C. Benack, T. Wang, K. Matthews, M.L. Taheri, Additive manufacturing methods for soft magnetic composites (SMCs), Microsc. Microanal. 24 (S1) (Aug 2018) 1066–1067, https://doi.org/10.1017/S1431927618005810.

[38] Evan Gaertner, Jennifer Rinker, Latha Sethuraman, Frederik Zahle, Benjamin Anderson, Definition of the IEA 15-Megawatt Offshore Reference Wind, National Renewable Energy Laboratory, Technical IEA Wind TCP Task 37, Mar 2020 [Online]. Available: https://www.nrel.gov/docs/fy20osti/75698.pdf. (Accessed 9 May 2020).

[39] A. Krings, M. Cossale, A. Tenconi, J. Soulard, A. Cavagnino, A. Boglietti, Magnetic materials used in electrical machines: a comparison and selection guide for early machine design, IEEE Ind. Appl. Mag. 23 (6) (Nov 2017) 21–28, https://doi.org/10.1109/MIAS.2016.2600721.

[40] T.N. Lamichhane, et al., Single-crystal permanent magnets: extraordinary magnetic behavior in the Ta-, Cu-, and Fe-substituted CeCo5 systems, Phys. Rev. Appl. 11 (1) (Jan 2019), https://doi.org/10.1103/PhysRevApplied.11.014052, p. 014052.

[41] T.N. Lamichhane, V. Taufour, A. Palasyuk, S.L. Bud'ko, P.C. Canfield, Study of the ferromagnetic quantum phase transition in Ce3−xMgxCo9, Philos. Mag. 100 (12) (Feb 2020) 1–13, https://doi.org/10.1080/14786435.2020.1727973.

[42] M. Javorski, J. Slavic, M. Boltezar, Frequency characteristics of magnetostriction in electrical steel related to the structural vibrations, IEEE Trans. Magn. 48 (12) (Dec 2012) 4727–4734, https://doi.org/10.1109/TMAG.2012.2203314.

[43] N. Bowler, Frequency-dependence of relative permeability in steel, AIP Conf. Proc. 820 (1) (Mar 2006) 1269–1276, https://doi.org/10.1063/1.2184670.

[44] A.M. Leary, P.R. Ohodnicki, M.E. McHenry, Soft magnetic materials in high-frequency, high-power conversion applications, JOM 64 (7) (Jul 2012) 772–781, https://doi.org/10.1007/s11837-012-0350-0.

[45] S. Somkun, A.J. Moses, P.I. Anderson, P. Klimczyk, Magnetostriction anisotropy and rotational magnetostriction of a nonoriented electrical steel, IEEE Trans. Magn. 46 (2) (Feb 2010) 302–305, https://doi.org/10.1109/TMAG.2009.2033123.

[46] J.M. Silveyra, E. Ferrara, D.L. Huber, T.C. Monson, Soft magnetic materials for a sustainable and electrified world, Science 362 (Oct 2018) 6413, https://doi.org/10.1126/science.aao0195.

[47] Soft Magnetic Applications Guide." Arnold Magnetic Technologies, [Online]. Available: https://www.arnoldmagnetics.com/wp-content/uploads/2017/10/FINAL_Tech-Library_Guides_Soft-Magnetics-Application-Guide.pdf.

[48] H.D. Arnold, G.W. Elmen, Permalloy, a new magnetic material of very high permeability, Bell Syst. Tech. J. 2 (3) (Jul 1923) 101–111, https://doi.org/10.1002/j.1538-7305.1923.tb03595.x.

[49] H.L.B. Gould, D.H. Wenny, Supermendur: a new rectangular-loop magnetic material, Electr. Eng. 76 (3) (Mar 1957) 208–211, https://doi.org/10.1109/EE.1957.6443037.

[50] TDK Corporation, "Ferrites and Accessories | Products | TDK Product Center." https://product.tdk.com/info/en/products/ferrite/index.html (accessed Dec. 19, 2019).

[51] K. Jalaiah, K.C. Mouli, R.V. Krishnaiah, K.V. Babu, P.S.V.S. Rao, The structural, DC resistivity and magnetic properties of Zr and Co co-substituted Ni0.5Zn0.5Fe2O4, Heliyon 5 (6) (Jun 2019): e01800, https://doi.org/10.1016/j.heliyon.2019.e01800.

[52] C. Ding, L. Liu, Y. Mei, K.D.T. Ngo, G.-Q. Lu, Magnetic paste as feedstock for additive manufacturing of power magnetics,", in: 2018 IEEE Applied Power Electronics Conference and Exposition (APEC), Mar 2018, pp. 615–618, https://doi.org/10.1109/APEC.2018.8341075.

[53] L. Liu, T. Ge, K.D.T. Ngo, Y. Mei, G. Lu, Ferrite paste cured with ultraviolet light for additive manufacturing of magnetic components for power electronics, IEEE Magn. Lett. 9 (2018) 1–5, https://doi.org/10.1109/LMAG.2018.2822622.

[54] I.H. Gul, A.Z. Abbasi, F. Amin, M. Anis-ur-Rehman, A. Maqsood, Structural, magnetic and electrical properties of Co1−xZnxFe2O4 synthesized by co-precipitation method, J. Magn. Magn. Mater. 311 (2) (Apr 2007) 494–499, https://doi.org/10.1016/j.jmmm.2006.08.005.

[55] I. Chicinas, V. Pop, O. Isnard, Synthesis of the supermalloy powders by mechanical alloying, J. Mater. Sci. 39 (16) (Aug 2004) 5305–5309, https://doi.org/10.1023/B:JMSC.0000039234.58490.78.

[56] A.K. Mazeeva, M.V. Staritsyn, V.V. Bobyr, S.A. Manninen, P.A. Kuznetsov, V.N. Klimov, Magnetic properties of Fe–Ni permalloy produced by selective laser melting, J. Alloys Compd. 814 (Jan 2020) 152315, https://doi.org/10.1016/j.jallcom.2019.152315.

[57] H. Schönrath, et al., Additive manufacturing of soft magnetic permalloy from Fe and Ni powders: control of magnetic anisotropy, J. Magn. Magn. Mater. 478 (May 2019) 274–278, https://doi.org/10.1016/j.jmmm.2018.11.084.

[58] 'Supermalloy': a new magnetic alloy, Nature 161 (4093) (Apr 1948) 554.

[59] C.V. Mikler, et al., Laser additive processing of Ni-Fe-V and Ni-Fe-Mo Permalloys: microstructure and magnetic properties, Mater. Lett. 192 (Apr 2017) 9–11, https://doi.org/10.1016/j.matlet.2017.01.059.

[60] C.V. Mikler, et al., Laser additive manufacturing of magnetic materials, JOM 69 (3) (Mar 2017) 532–543, https://doi.org/10.1007/s11837-017-2257-2.

[61] Lamichhane T. et al., Comparative study of SLM and BJT processed Fe-3Si alloys.

[62] C.L. Cramer, et al., Binder jet additive manufacturing method to fabricate near net shape crack-free highly dense Fe-6.5 wt.% Si soft magnets, Heliyon 5 (11) (Nov 2019): e02804, https://doi.org/10.1016/j.heliyon.2019.e02804.

[63] Soft Magnetic Applications Guide, Arnold MagneticTechnologies, SMGA, 2015 a.

[64] A.B. Kustas, et al., Characterization of the Fe-Co-1.5V soft ferromagnetic alloy processed by laser engineered net shaping (LENS), Addit. Manuf. 21 (May 2018) 41–52, https://doi.org/10.1016/j.addma.2018.02.006.

[65] A.B. Kustas, C.M. Fancher, S.R. Whetten, D.J. Dagel, J.R. Michael, D.F. Susan, Controlling the extent of atomic ordering in intermetallic alloys through additive manufacturing, Addit. Manuf. 28 (Aug 2019) 772–780, https://doi.org/10.1016/j.addma.2019.06.020.

[66] Y.G. Nam, et al., Selective laser melting vitrification of amorphous soft magnetic alloys with help of double-scanning-induced compositional homogeneity, Mater. Lett. 261 (Feb 2020) 127068, https://doi.org/10.1016/j.matlet.2019.127068.

[67] T. Gheiratmand, H.R. Madaah Hosseini, P. Davami, C. Sarafidis, Fabrication of FINEMET bulk alloy from amorphous powders by spark plasma sintering, Powder Technol. 289 (Feb 2016) 163–168, https://doi.org/10.1016/j.powtec.2015.11.060.

[68] Y. Yoshizawa, S. Oguma, K. Yamauchi, New Fe-based soft magnetic alloys composed of ultrafine grain structure, J. Appl. Phys. 64 (10) (Nov 1988) 6044–6046, https://doi.org/10.1063/1.342149.

[69] Learn about Magnetic Materials from Metglas®, Inc.," Metglas, Inc. https://metglas.com/magnetic-materials/(accessed May 18, 2020).

[70] Paul Ohodnicki, "Soft Magnetic Alloys for Electrical Machine Applications: Basics, State-Of-The-Art, and R&D Opportunities." National Energy Technology Center, Accessed: Apr. 20, 2020. [Online]. Available: https://www.nist.gov/system/files/documents/pml/high_megawatt/Ohodnicki-DOE_SoftMagneticMaterialsForElectricMachines_NIST_Ohodnicki_9_10_2015.pdf.

[71] H. Shokrollahi, K. Janghorban, Soft magnetic composite materials (SMCs), J. Mater. Process. Technol. 189 (1) (2007) 1–12, https://doi.org/10.1016/j.jmatprotec.2007.02.034.

[72] A. Kallaste, T. Vaimann, A. Rassälkin, Additive Design Possibilities of Electrical Machines, in: 2018 IEEE 59th International Scientific Conference on Power and Electrical Engineering of Riga Technical University (RTUCON), Nov 2018, pp. 1–5, https://doi.org/10.1109/RTUCON.2018.8659828.

[73] H. Fayazfar, et al., A critical review of powder-based additive manufacturing of ferrous alloys: process parameters, microstructure and mechanical properties, Mater. Des. 144 (Apr 2018) 98–128, https://doi.org/10.1016/j.matdes.2018.02.018.

[74] S. Urbanek, et al., Additive manufacturing of a soft magnetic rotor active part and shaft for a permanent magnet synchronous machine, in: 2018 IEEE Transportation Electrification Conference and Expo (ITEC), Jun 2018, pp. 668–674, https://doi.org/10.1109/ITEC.2018.8450250.

[75] T.Q. Pham, T.T. Do, P. Kwon, S.N. Foster, Additive manufacturing of high performance ferromagnetic materials, in: 2018 IEEE Energy Conversion Congress and Exposition (ECCE), Sep 2018, pp. 4303–4308, https://doi.org/10.1109/ECCE.2018.8558245.

[76] H.-S. Hong, H.-C. Liu, S.-Y. Cho, J. Lee, C.-S. Jin, Design of high-end synchronous reluctance motor using 3-D printing technology, IEEE Trans. Magn. 53 (6) (Jun 2017) 1–5, https://doi.org/10.1109/TMAG.2017.2659782.

[77] L.M. Bollig, P.J. Hilpisch, G.S. Mowry, B.B. Nelson-Cheeseman, 3D printed magnetic polymer composite transformers, J. Magn. Magn. Mater. 442 (Nov 2017) 97–101, https://doi.org/10.1016/j.jmmm.2017.06.070.

[78] Y. Yan, Design Methodology and Materials for Additive Manufacturing of Magnetic Components, Apr 2017 [Online]. Available: https://vtechworks.lib.vt.edu/handle/10919/77394. (Accessed 3 January 2020).

[79] R. Wrobel, A. Hussein, Design considerations of heat guides fabricated using additive manufacturing for enhanced heat transfer in electrical machines,, in: 2018 IEEE Energy Conversion Congress and Exposition (ECCE), Sep 2018, pp. 6506–6513, https://doi.org/10.1109/ECCE.2018.8557559.

[80] E.A. Périgo, J. Jacimovic, F. García Ferré, L.M. Scherf, Additive manufacturing of magnetic materials, Addit. Manuf. 30 (Dec 2019) 100870, https://doi.org/10.1016/j.addma.2019.100870.

[81] T. Niendorf, S. Leuders, A. Riemer, H.A. Richard, T. Tröster, D. Schwarze, Highly anisotropic steel processed by selective laser melting, Metall. Mater. Trans. B 44 (4) (Aug 2013) 794–796, https://doi.org/10.1007/s11663-013-9875-z.

[82] L. Thijs, K. Kempen, J.-P. Kruth, J. Van Humbeeck, Fine-structured aluminium products with controllable texture by selective laser melting of pre-alloyed AlSi10Mg powder, Acta Mater. 61 (5) (Mar 2013) 1809–1819, https://doi.org/10.1016/j.actamat.2012.11.052.

[83] B. Li, W. Fu, H. Xu, B. Qian, F. Xuan, Additively manufactured Ni-15Fe-5Mo Permalloy via selective laser melting and subsequent annealing for magnetic-shielding structures: process, micro-structural and soft-magnetic characteristics, J. Magn. Magn. Mater. 494 (Jan 2020) 165754, https://doi.org/10.1016/j.jmmm.2019.165754.

[84] I. Shishkovsky, V. Saphronov, Peculiarities of selective laser melting process for permalloy powder, Mater. Lett. 171 (May 2016) 208–211, https://doi.org/10.1016/j.matlet.2016.02.099.
[85] T. Riipinen, S. Metsä-Kortelainen, T. Lindroos, J.S. Keränen, A. Manninen, J. Pippuri-Mäkeläinen, Properties of soft magnetic Fe-Co-V alloy produced by laser powder bed fusion, Rapid Prototyp. J. 25 (4) (Jan 2019) 699–707, https://doi.org/10.1108/RPJ-06-2018-0136.
[86] A. Páez-Pavón, A. Jiménez-Morales, M. Rodriguez-Arbaizar, E. Carreño-Morelli, J.M. Torralba, "Sintering optimisation of Fe–Si soft magnetic materials processed by metal injection moulding, Powder Metall. 60 (2) (Mar 2017) 112–119, https://doi.org/10.1080/00325899.2017.1289631.
[87] N. D. Watson and P. V. Lockette, "Deposition Controlled Magnetic Alignment in Iron-PLA Composites," p. 7.
[88] B. Khatri, K. Lappe, D. Noetzel, K. Pursche, T. Hanemann, "A 3D-printable polymer-metal soft-magnetic functional composite—development and characterization, Materials 11 (2) (Jan 2018), https://doi.org/10.3390/ma11020189.
[89] C. Huber, et al., Additive manufactured and topology optimized passive shimming elements for permanent magnetic systems, Sci. Rep. 8 (1) (Oct 2018) 1–8, https://doi.org/10.1038/s41598-018-33059-w.
[90] G. Chatzipirpiridis, et al., 3D printing of thermoplastic-bonded soft- and hard-magnetic composites: magnetically tuneable architectures and functional devices, Adv. Intell. Syst. 1 (6) (2019) 1900069, https://doi.org/10.1002/aisy.201900069.
[91] R. De Santis, U. D'Amora, T. Russo, A. Ronca, A. Gloria, L. Ambrosio, 3D fibre deposition and stereolithography techniques for the design of multifunctional nanocomposite magnetic scaffolds, J. Mater. Sci. Mater. Med. 26 (10) (Sep 2015) 250, https://doi.org/10.1007/s10856-015-5582-4.
[92] L.M. Bollig, M.V. Patton, G.S. Mowry, B.B. Nelson-Cheeseman, Effects of 3-D printed structural characteristics on magnetic properties, IEEE Trans. Magn. 53 (11) (Nov 2017) 1–6, https://doi.org/10.1109/TMAG.2017.2698034.
[93] X.-N. Guan, X.-N. Xu, R. Kuniyoshi, H.-H. Zhou, Y.-F. Zhu, Electromagnetic and mechanical properties of carbonyl iron powders-PLA composites fabricated by fused deposition modeling, Mater. Res. Express 5 (11) (Sep 2018) 115303, https://doi.org/10.1088/2053-1591/aadce4.
[94] A.H. Morgenstern, T.M. Calascione, N.A. Fischer, T.J. Lee, J.E. Wentz, B.B. Nelson-Cheeseman, Thermoplastic magnetic elastomer for fused filament fabrication, AIMS Mater. Sci. 6 (May 2019) 363–376, https://doi.org/10.3934/matersci.2019.3.363.
[95] M.P. Caputo, A.E. Berkowitz, A. Armstrong, P. Müllner, C.V. Solomon, 4D printing of net shape parts made from Ni-Mn-Ga magnetic shape-memory alloys, Addit. Manuf. 21 (May 2018) 579–588, https://doi.org/10.1016/j.addma.2018.03.028.
[96] T.Q. Pham, H. Suen, P. Kwon, S.N. Foster, Characterization of magnetic anisotropy for binder jet printed Fe93.25Si6.75,, in: 2019 IEEE Energy Conversion Congress and Exposition (ECCE), Sep 2019, pp. 745–752, https://doi.org/10.1109/ECCE.2019.8913105.
[97] E. Peng, X. Wei, T.S. Herng, U. Garbe, D. Yu, J. Ding, Ferrite-based soft and hard magnetic structures by extrusion free-forming, RSC Adv. 7 (43) (May 2017) 27128–27138, https://doi.org/10.1039/C7RA03251J.
[98] C. Cuchet, A. Muster, P. Germano, Y. Perriard, Soft magnets implementation using a stereolithography-based 3D printer, in: 2017 20th International Conference on Electrical Machines and Systems (ICEMS), Aug 2017, pp. 1–5, https://doi.org/10.1109/ICEMS.2017.8056301.
[99] Z. Ji, C. Yan, B. Yu, X. Wang, F. Zhou, Multimaterials 3D printing for free assembly manufacturing of magnetic driving soft actuator, Adv. Mater. Interfaces 4 (22) (2017) 1700629, https://doi.org/10.1002/admi.201700629.
[100] M. Garibaldi, I. Ashcroft, M. Simonelli, R. Hague, Metallurgy of high-silicon steel parts produced using Selective Laser Melting, Acta Mater. 110 (May 2016) 207–216, https://doi.org/10.1016/j.actamat.2016.03.037.
[101] G. Ouyang, et al., Effect of wheel speed on magnetic and mechanical properties of melt spun Fe-6.5 wt.% Si high silicon steel, AIP Adv. 8 (5) (Dec 2017): 056111, https://doi.org/10.1063/1.5006481.
[102] Y. Takada, M. Abe, S. Masuda, J. Inagaki, "Commercial scale production of Fe-6.5 wt.% Si sheet and its magnetic properties, J. Appl. Phys. 64 (10) (Nov 1988) 5367–5369, https://doi.org/10.1063/1.342373.
[103] H. Haiji, K. Okada, T. Hiratani, M. Abe, M. Ninomiya, Magnetic properties and workability of 6.5% Si steel sheet, in: Proc. Twelfth Int. Conf. Soft Magn. Mater., vol. 160, Jul 1996, pp. 109–114, https://doi.org/10.1016/0304-8853(96)00128-X.
[104] M. Garibaldi, I. Ashcroft, J.N. Lemke, M. Simonelli, R. Hague, Effect of annealing on the microstructure and magnetic properties of soft magnetic Fe-Si produced via laser additive manufacturing, Scripta Mater. 142 (2018) 121–125, https://doi.org/10.1016/j.scriptamat.2017.08.042.
[105] J.N. Lemke, et al., Calorimetric study and microstructure analysis of the order-disorder phase transformation in silicon steel built by SLM, J. Alloys Compd. 722 (Oct 2017) 293–301, https://doi.org/10.1016/j.jallcom.2017.06.085.
[106] G.P. Dinda, A.K. Dasgupta, J. Mazumder, "Evolution of microstructure in laser deposited Al–11.28%Si alloy, Surf. Coat. Technol. 206 (8) (Jan 2012) 2152–2160, https://doi.org/10.1016/j.surfcoat.2011.09.051.
[107] S. Simizu, P.R. Ohodnicki, M.E. McHenry, Metal amorphous nanocomposite soft magnetic material-enabled high power density, rare earth free rotational machines, IEEE Trans. Magn. 54 (5) (May 2018) 1–5, https://doi.org/10.1109/TMAG.2018.2794390.
[108] Permalloy | Metallurgy," Encyclopedia Britannica. https://www.britannica.com/technology/Permalloy (accessed Dec. 18, 2019).
[109] Bell Telephone Laboratories, Permalloy, J. Chem. Educ. 2 (12) (Dec 1925) 1157, https://doi.org/10.1021/ed002p1157.
[110] G.W. Elmen, Magnetic alloys of iron, nickel, and cobalt*, Bell Syst. Tech. J. 15 (1) (1936) 113–135, https://doi.org/10.1002/j.1538-7305.1936.tb00721.x.
[111] Y. Arbaoui, et al., 3D printed ferromagnetic composites for microwave applications, J. Mater. Sci. 52 (9) (May 2017) 4988–4996, https://doi.org/10.1007/s10853-016-0737-3.
[112] Y. Yan, J. Moss, K.D.T. Ngo, Y. Mei, G.-Q. Lu, Additive manufacturing of toroid inductor for power electronics applications, IEEE Trans. Ind. Appl. 53 (6) (Nov 2017) 5709–5714, https://doi.org/10.1109/TIA.2017.2729504.
[113] Y. Yan, K.D.T. Ngo, Yuhui Mei, Guo-Quan Lu, Additive manufacturing of magnetic components for power electronics integration, in: 2016 International Conference on Electronics Packaging (ICEP), Apr 2016, pp. 368–371, https://doi.org/10.1109/ICEP.2016.7486849.
[114] R.V. Major, C.M. Orrock, High saturation ternary cobalt-iron basalt alloys, IEEE Trans. Magn. 24 (2) (Mar 1988) 1856–1858, https://doi.org/10.1109/20.11625.
[115] N.X. Sun, S.X. Wang, Soft high saturation magnetization (Fe/sub 0.7/Co/sub 0.3/)/sub 1-x/N/sub x/thin films for inductive write heads, IEEE Trans. Magn. 36 (5) (Sep 2000) 2506–2508, https://doi.org/10.1109/20.908488.
[116] R.S. Sundar, S.C. Deevi, Soft magnetic FeCo alloys: alloy development, processing, and properties, Int. Mater. Rev. 50 (3) (Jun 2005) 157–192, https://doi.org/10.1179/174328005X14339.
[117] Y. Ustinovshikov, S. Tresheva, Character of transformations in Fe–Co system, Mater. Sci. Eng. A 248 (1) (Jun 1998) 238–244, https://doi.org/10.1016/S0921-5093(98)00506-1.
[118] A.H. Tkaczyk, A. Bartl, A. Amato, V. Lapkovskis, M. Petranikova, Sustainability evaluation of essential critical raw materials: cobalt, niobium, tungsten and rare earth elements, J. Phys. Appl. Phys. 51 (20) (Apr 2018) 203001, https://doi.org/10.1088/1361-6463/aaba99.
[119] X. Yang, et al., Effect of remelting on microstructure and magnetic properties of Fe-Co-based alloys produced by laser additive manufacturing, J. Phys. Chem. Solid. 130 (Jul 2019) 210–216, https://doi.org/10.1016/j.jpcs.2019.03.001.
[120] J. Geng, I.C. Nlebedim, M.F. Besser, E. Simsek, R.T. Ott, Bulk combinatorial synthesis and high throughput characterization for rapid assessment of magnetic materials: application of laser engineered net shaping (LENS^{TM}), JOM 68 (7) (Jul 2016) 1972–1977, https://doi.org/10.1007/s11837-016-1918-x.
[121] X. Yang, X. Cui, G. Jin, J. Liu, Y. Chen, Z. Liu, Soft magnetic property of (Fe60Co35Ni5)78 Si6B12Cu1Mo3 alloys by laser additive manufacturing, J. Magn. Magn. Mater. 466 (Nov 2018) 75–80, https://doi.org/10.1016/j.jmmm.2018.06.085.
[122] R. Hasegawa, Design and fabrication of new soft magnetic materials, J. Non-Cryst. Solids 329 (1) (Nov 2003) 1–7, https://doi.org/10.1016/j.jnoncrysol.2003.08.002.
[123] S. Yoshida, T. Mizushima, T. Hatanai, A. Inoue, Preparation of new amorphous powder cores using Fe-based glassy alloy, IEEE Trans. Magn. 36 (5) (Sep 2000) 3424–3429, https://doi.org/10.1109/20.908848.
[124] R. Conteri, et al., Laser additive processing of Fe-Si-B-Cu-Nb magnetic alloys, J. Manuf. Process. 29 (Oct 2017) 175–181, https://doi.org/10.1016/j.jmapro.2017.07.029.
[125] T. Borkar, R. Conteri, X. Chen, R.V. Ramanujan, R. Banerjee, Laser additive processing of functionally-graded Fe–Si–B–Cu–Nb soft magnetic materials, Mater. Manuf. Process. 32 (14) (Oct 2017) 1581–1587, https://doi.org/10.1080/10426914.2016.1244849.
[126] S.J. Louis, B. Jan, L.M. Willem, Manganese Zinc Ferrite Core, May 8 1951. US2551711A.
[127] Ferroxcube, "Download-Ferroxcube." https://www.ferroxcube.com/en-global/download/index (accessed Dec. 19, 2019).
[128] KEMET Corporation, "EMC," Engineering Center. https://ec.kemet.com/emc/ (accessed Dec. 19, 2019).
[129] The Biggest & Most Expensive 3D Printers in the World, Jan 22 2018. All3DP, https://all3dp.com/1/biggest-large-3d-printer-world-most-expensive/. (Accessed 23 June 2020).
[130] D.L. Bourell, H.L. Marcus, J.W. Barlow, J.J. Beaman, Selective laser sintering of metals and ceramics, Int. J. Powder Metall. Princeton, N.J. 28 (4) (Oct 1992) 369–381.
[131] H. Tiismus, A. Kallaste, T. Vaimann, A. Rassölkin, A. Belahcen, Electrical resistivity of additively manufactured silicon steel for electrical machine fabrication, in: 2019 Electric Power Quality and Supply Reliability Conference (PQ) 2019 Symposium on Electrical Engineering and Mechatronics (SEEM), Jun 2019, pp. 1–4, https://doi.org/10.1109/PQ.2019.8818252.
[132] M. Garibaldi, Laser Additive Manufacturing of Soft Magnetic Cores for Rotating Electrical Machinery: Materials Development and Part Design, Dec 12 2018. http://eprints.nottingham.ac.uk/52326/. (Accessed 14 March 2020).
[133] B. Zhang, Y. Li, Q. Bai, Defect formation mechanisms in selective laser melting: a review, Chin. J. Mech. Eng. 30 (3) (May 2017) 515–527, https://doi.org/10.1007/s10033-017-0121-5.
[134] WNLO Unveils China's Largest SLM 3D Printer for Production of Metal Parts, 3ders.org. http://www.3ders.org/articles/20160506-wnlo-unveils-chinas-largest-slm-3d-printer-for-production-of-metal-parts.html (accessed Mar. 13, 2020).

[135] Fraunhofer Opens 'World's Largest SLM Facility' in Aachen Germany, 3D Printing Industry, https://3dprintingindustry.com/news/fraunhofer-opens-worlds-largest-slm-facility-aachen-germany-115961/, Jun 14 2017. (Accessed 13 March 2020).
[136] L. Li, B. Post, V. Kunc, A.M. Elliott, M.P. Paranthaman, Additive manufacturing of near-net-shape bonded magnets: prospects and challenges, Scripta Mater. 135 (2017) 100–104, https://doi.org/10.1016/j.scriptamat.2016.12.035.
[137] German Researchers Showcase Electric Motor Produced Entirely by Additive Manufacturing, May 7 2018. Metal Additive Manufacturing, https://www.metal-am.com/german-researchers-showcase-electric-motor-produced-entirely-by-additive-manufacturing/. (Accessed 10 March 2020).
[138] B. Post et al., "Big area additive manufacturing application in wind turbine molds," CRADA FINAL REPORT NFE-16-06051. [Online]. Available: https://info.ornl.gov/sites/publications/Files/Pub75291.pdf.
[139] WHAM, There's a New 'largest 3D Printer in the World' in Town, Oct 1 2018, 3D Printing Media Network, https://www.3dprintingmedia.network/wham-theres-a-new-largest-composite-3d-printer-in-the-world-in-town/. (Accessed 13 March 2020).
[140] University of Maine Creates the World's Largest 3D Printed Boat, Oct 16 2019, 3Dnatives, https://www.3dnatives.com/en/3d-printed-boat-university-of-maine-161020195/. (Accessed 13 March 2020).
[141] S. Mirzababaei, S. Pasebani, A review on binder jet additive manufacturing of 316L stainless steel, J. Manuf. Mater. Process. 3 (3) (Sep 2019) 82, https://doi.org/10.3390/jmmp3030082.
[142] VX1000 | Voxeljet 3D Printing Systems, voxeljet.Com. https://www.voxeljet.com/3d-drucksysteme/vx1000/(accessed Mar. 13, 2020).
[143] M. Feygin, S.S. Pak, Laminated object manufacturing apparatus and method, Mar 2 1999. US5876550A.
[144] M. Feygin, A. Shkolnik, M.N. Diamond, E. Dvorskiy, Laminated object manufacturing system, Mar 24 1998. US5730817A.
[145] MOTORPRINTER, Best Electric Machine. https://bestelectricmachine.com/motorprinter-details/(accessed May 15, 2020).
[146] J. Yoo, N. Kikuchi, Topology optimization in magnetic fields using the homogenization design method, Int. J. Numer. Methods Eng. 48 (10) (2000) 1463–1479, https://doi.org/10.1002/1097-0207(20000810)48:10<1463::AID-NME9>3.0.CO;2-552.
[147] S. Shamshirband, T. Rabczuk, K.-W. Chau, A survey of deep learning techniques: application in wind and solar energy resources, IEEE Access 7 (2019) 164650–164666, https://doi.org/10.1109/ACCESS.2019.2951750.
[148] M. Ganjkhani, S.N. Fallah, S. Badakhshan, S. Shamshirband, K. Chau, A novel detection algorithm to identify false data injection attacks on power system state estimation, Energies 12 (11) (Jan 2019) 2209, https://doi.org/10.3390/en12112209.
[149] D. Wang, et al., The effect of a scanning strategy on the residual stress of 316L steel parts fabricated by selective laser melting (SLM), Materials 11 (Sep 2018) 10, https://doi.org/10.3390/ma11101821.
[150] S.N. Fallah, M. Ganjkhani, S. Shamshirband, K. Chau, Computational intelligence on short-term load Forecasting: a methodological overview, Energies 12 (3) (Jan 2019) 393, https://doi.org/10.3390/en12030393.
[151] A. Dineva, A. Mosavi, M. Gyimesi, I. Vajda, N. Nabipour, T. Rabczuk, Fault diagnosis of rotating electrical machines using multi-label classification, Appl. Sci. 9 (23) (Jan 2019) 5086, https://doi.org/10.3390/app9235086.
[152] D. Ganga, V. Ramachandran, Adaptive prediction model for effective electrical machine maintenance, J. Qual. Mainten. Eng. 26 (1) (Jan 2019) 166–180, https://doi.org/10.1108/JQME-12-2017-0087.
[153] N. R. C. Canada, NRC capabilities in advanced manufacturing, Apr 1 2019. https://nrc.canada.ca/en/research-development/research-collaboration/programs/nrc-capabilities-advanced-manufacturing. (Accessed 23 April 2020).
[154] J. Kolehmainen, J. IkÄheimo, Motors with buried magnets for medium-speed applications, IEEE Trans. Energy Convers. 23 (1) (Mar 2008) 86–91, https://doi.org/10.1109/TEC.2007.914331.
[155] V.V. Popov, A. Fleisher, Hybrid additive manufacturing of steels and alloys, Manuf. Rev. 7 (2020) 6, https://doi.org/10.1051/mfreview/2020005.
[156] R.R. Ma, J.T. Belter, A.M. Dollar, Hybrid deposition manufacturing: design strategies for multimaterial mechanisms via three-dimensional printing and material deposition, J. Mech. Robot. 7 (2) (May 2015), https://doi.org/10.1115/1.4029400.
[157] M.P. Sealy, G. Madireddy, R.E. Williams, P. Rao, M. Toursangsaraki, Hybrid processes in additive manufacturing, J. Manuf. Sci. Eng. 140 (6) (Jun 2018), https://doi.org/10.1115/1.4038644.
[158] L. Li, A. Haghighi, Y. Yang, A novel 6-axis hybrid additive-subtractive manufacturing process: design and case studies, J. Manuf. Process. 33 (Jun 2018) 150–160, https://doi.org/10.1016/j.jmapro.2018.05.008.
[159] C. Subramaniam, et al., "One hundred fold increase in current carrying capacity in a carbon nanotube–copper composite, Nat. Commun. 4 (1) (Jul 2013) 2202, https://doi.org/10.1038/ncomms3202.
[160] V. Rallabandi, N. Taran, D.M. Ionel, J.F. Eastham, On the feasibility of carbon nanotube windings for electrical machines — case study for a coreless axial flux motor, in: 2016 IEEE Energy Conversion Congress and Exposition (ECCE), Sep 2016, pp. 1–7, https://doi.org/10.1109/ECCE.2016.7855306.
[161] D. Zhang, et al., Fabrication of highly conductive graphene flexible circuits by 3D printing, Synth. Met. 217 (Jul 2016) 79–86, https://doi.org/10.1016/j.synthmet.2016.03.014.
[162] T. El-Wardany, Y. She, V. Jagdale, J.K. Garofano, J. Liou, W. Schmidt, Challenges in 3D printing of high conductivity copper, in: Presented at the ASME 2017 International Technical Conference and Exhibition on Packaging and Integration of Electronic and Photonic Microsystems Collocated with the ASME 2017 Conference on Information Storage and Processing Systems, Oct 2017, https://doi.org/10.1115/IPACK2017-74306.
[163] T.Q. Tran, et al., 3D printing of highly pure copper, Metals 9 (7) (Jul 2019) 756, https://doi.org/10.3390/met9070756.